DESIGN AND DEVELOPMENT OF ORGANOLEAD HALIDE PEROVSKITE SOLAR CELLS

by

Beyza Yılmaz

B.S., Chemical Engineering, Boğaziçi University, 2015

Submitted to the Institute for Graduate Studies in
Science and Engineering in partial fulfillment of
the requirements for the degree of
Master of Science

Graduate Program in Chemical Engineering
Boğaziçi University
2017

ACKNOWLEDGEMENTS

First, I would like to express my great appreciation to my thesis supervisor, Prof. Ramazan Yıldırım for his guidance, support, and encouragement during my thesis. It was a privilege for me to work with him during my graduate study.

I would like to thank my thesis committee members, Prof. Ahmet Erhan Aksoylu and Assist. Prof. Mehmet Erdem Günay for sparing their valuable time and for their contributions.

I also would like to thank to Dr. Bilge Gedik Uluocak for her valuable time and effort in SEM analyses and Sputtering processes performed at Boğaziçi University Advanced Technologies Research and Development Center.

I have special thanks to Çağla Odabaşı who helped me to improve my work, her advices were invaluable for me.

I have very special thanks to my friends Elif Can, Elif Gençtürk and Burcu Acar for their sincere friendship and mental support. I feel very lucky to have them I also want to thank my laboratory friends, CATREL team and all ChE members.

Finally, I want to thank my family for their love, endless patience, continuous support, and encouragement in my whole life.

This thesis is supported by Boğaziçi University Research Fund through Project 16A05TUG2.

ABSTRACT

DESIGN AND DEVELOPMENT OF ORGANOLEAD HALIDE PEROVSKITE SOLAR CELLS

The aim of this thesis was to design and develop organolead halide perovskite solar cells by employing cost efficient and easily generated materials via industrially applicable processes. In the experiments, two kinds of perovskite solar cells were fabricated in terms of their device configurations. First, TiO_2 electron transport material based n-i-p type planar perovskite solar cells were produced. Using both single and sequential deposition techniques, methylammonium lead iodide ($MAPbI_3$) perovskite was coated on TiO_2. PCBM and ZnO charge carriers were applied on perovskite surface by spin coating. The PSCs were completed with the addition of Al and Cu conductive tapes as back contact of the device. The other design was inverted planar PSC. This device was fabricated based on p-type NiO conductive material. NiO was spun on ITO substrates as hole transporting material. The second layer of the device was also $MAPbI_3$ perovskite which was synthesized by both one-step and two-step deposition methods. However, one-step deposited PSCs with NiO as HTM did not work due to insufficient surface coverage. The next step was the coating of ZnO and ionic liquid electron transport materials on perovskite crystals. On the other hand, ETL-free solar cells were also fabricated. All devices with NiO as HTM were finished with attachment of Al and Cu tapes which were the back electrode of the structure. In addition, NiO/$MAPbI_3$/ZnO configurated device was arranged to contain Au electrode deposited by sputtering method. All coating operations were performed by spin coating method under ambient conditions. The PSCs were measured by using Keithley 2401 Source Meter at 100 mW/cm^2 irradiance of ABET LS 150 Xenon Lamp Source solar simulator. The PSC with the best efficiency which was 7.27×10^{-3}% had the configuration as NiO/$MAPbI_3$/ZnO/Al. Moreover, this device demonstrated electrical characteristics of 0.51 V open circuit voltage, 27.3% fill factor and 0.052 mA/cm^2 short circuit current density. The results are very low compared to literature due to perovskite degradation originated from high humidity of air.

ÖZET

ORGANİK KURŞUN HALOJENÜR PEROVSKİT GÜNEŞ HÜCRELERİNİN DİZAYNI VE GELİŞTİRİLMESİ

Bu tezin amacı, organik kurşun halojenür perovskit güneş hücrelerinin ucuz maliyetli ve kolay sentezlenebilir malzemelerle endüstride uygulanılabilecek süreçler kullanılarak tasarlanması ve geliştirilmesidir. Deneylerde, iki farklı yapıda perovskit hücre yapılmıştır. İlk olarak, TiO_2 elektron taşıyıcılı n-i-p tipi düzlemsel perovskit güneş hücreleri üretilmiştir. Metilamonyum kurşun iyodür ($MAPbI_3$) perovskit tek ve iki aşamalı sentez yöntemi kullanılarak TiO_2 üzerine kaplanmıştır. PCBM ve ZnO yük taşıyıcıları perovskit yüzeyine dönel kaplama yöntemi kullanılarak uygulanmıştır. Perovskit güneş hücreleri Al ve Cu iletken bantlarının arka elektrot olarak eklenmesiyle tamamlanmıştır. Bir diğer hücre tasarımı p-i-n tipi tersine çevrilmiş düzlemsel yapıdadır. Bu yapıdaki cihazlar p-tipi olan NiO iletken malzeme bağlı kalınarak üretilmiştir. NiO, ITO ön elektrotu üzerine deşik taşıyıcı olarak kaplanmıştır. Hücrenin ikinci tabakası tek ve çift aşamalı olarak sentezlenen $MAPbI_3$ perovskit malzemeden oluşmaktadır. Ancak, tek aşamalı olarak sentezlenen NiO deşik taşıyıcılı perovskit güneş hücresi perovskit yüzey kaplamasının yetersizliği sebebiyle çalışmamıştır. Bir sonraki aşama perovskit kristalleri üzerine ZnO ve iyonik sıvı elektron taşıyıcı malzemelerinin kaplanmasıdır. Öte yandan, elektron taşıyıcı tabakası olmayan hücreler de üretilmiştir. NiO deşik taşıyıcılı hücrelerin hepsi, Al ve Cu iletken bantlarının arka elektrot olarak eklenmesiyle tamamlanmıştır. Buna ek olarak, $NiO/MAPbI_3/ZnO$ dizilimine sahip hücreler, sıçratma (sputtering) ile oluşturulmuş Au elektrotu içerecek şekilde düzenlenmiştir. Kaplama işlemlerinin tamamı dönel kaplama metodu kullanılarak çevre şartları altında uygulanmıştır. Perovskit güneş hücrelerinin ölçümleri Keithley 2401 Source Meter cihazıyla 100 mW/cm^2 gücünde ABET LS 150 Xenon Lamp Source güneş simülatörü kullanılarak yapılmıştır. $NiO/MAPbI_3/ZnO/Al$ yapılı perovskit güneş hücresi $\%7.27\times10^{-3}$ ile en yüksek verime sahiptir. Ayrıca, hücre 0.51V açık devre voltajı, %27.3 FF ve 0.052 mA/cm^2 kısa devre akım yoğunluğu değerlerini göstermiştir. Sonuçlar, havadaki nemin perovskit yapısını bozması sebebiyle literatüre göre oldukça düşük çıkmıştır.

TABLE OF CONTENTS

LIST OF FIGURES

LIST OF TABLES

LIST OF SYMBOLS

I_{SC}	Short circuit current	mA
I_{MP}	Current at maximum power point	mA
J_{SC}	Short circuit current density	mA/cm^2
P_{light}	Power of light	W
P_{max}	Maximum Power	W
V_{MP}	Voltage at maximum power point	V
V_{OC}	Open circuit voltage	V
η	Power conversion efficiency	

LIST OF ACRONYMS/ABBREVIATIONS

2D	Two Dimensional
3D	Three Dimensional
AM	Air Mass
CIGS	Copper Indium Gallium Diselenide
CBM	Conduction Band Minimum
DMF	N, N-Dimethylformamide
DMSO	Dimethyl Sulfoxide
ETL	Electron Transport Layer
ETM	Electron Transport Material
$FAPbI_3$	Formamidinium Lead Iodide
FF	Fill Factor
FTO	Fluorine doped Tin Oxide
GBL	Gamma (γ)-Butyrolactone
HOMO	Highest Occupied Molecular Orbital
HTL	Hole Transport Layer
HTM	Hole Transport Material
IL	Ionic Liquid
ITO	Indium Tin Oxide
LBSO	Lanthanum (La)-doped $BaSnO_3$
Li-TFSI	Lithium bis(trifluoromethylsulphonyl) imide
LUMO	Lowest Unoccupied Molecular Orbital
MAI	Methylammonium Iodide
$MAPbI_3$	Methylammonium Lead Iodide
NREL	National Renewable Energy Laboratory
PCE	Power Conversion Efficiency
PSC	Perovskite Solar Cell
TBP	4-tertbutylpyridine
VBM	Valance Band Maximum

1. INTRODUCTION

The decline in the oil sources and the ascending need for energy have been created a global energy problem in recent years; most of the energy required is produced from fossil fuels either from petroleum, natural gas, or coal, which causes greenhouse effect and global warming. Therefore, both the depletion of fuels and ecological factors lead to search for more environmentally friendly alternative energy sources to replace the conventional energy solutions (Grätzel and Zakeeruddin, 2013; Bella, 2015).

Solar energy is a clean, abundant, and renewable energy source, which can meet global energy demand in future (Grätzel and Zakeeruddin, 2013). The energy that Sun can provide to Earth is so massive that the solar energy absorbed by Earth in one hour is higher than the recent global annual energy consumption (Bella, 2015). So, there is a great potential of the solar energy applications to satisfy the global energy demand.

Photovoltaic devices can directly transform the solar energy into electrical energy. Therefore, photovoltaics have been regarded as the most significant technology to overcome the high energy problem of the world. Silicon technology was the leading applications in photovoltaics (Grätzel and Zakeeruddin, 2013); however, more efficient, and cheaper methods are required. Over the last two decades, scientists have focused on the development of the new photovoltaic devices which can efficiently convert solar energy into electricity (Bella, 2015). Nowadays, the new applications for photovoltaics is arising as third generation or emerging technologies. The purpose of these technologies is to attain high efficiency of photovoltaics by employing cheap, harmless, and widely available materials (Bella, 2015).

The third-generation solar cells include dye-sensitized solar cells, quantum dot solar cells, organic solar cells, and inorganic/organic perovskite solar cells. These emerging technologies have been extensively studied to fabricate low-cost, highly efficient, and elastic devices (Jeon *et al*., 2014). The target is to develop solar cells which can be produced as large scale in industry (Bella, 2015). Easier methods and simple materials are preferred to be successful in industrial processes. Perovskite solar cells are one of the improving photovoltaics among the third-generation solar cells (Chen *et al*., 2013). The power

conversion efficiency of perovskite solar cells has reached up to 21.2 % which is a considerably high performance for a developing technology (Shin *et al*., 2017).

Perovskite is recently one of the most popular materials as an absorber medium for thin film solar cells. Due to perovskite's properties which are proper band gap, high absorption coefficient, successful electron movement and high tolerance for defects, the power conversion efficiency of perovskite solar cells increased rapidly. In addition to their ease of fabrication, perovskites have relatively low cost (Chen *et al*., 2013).

The first usage of the organolead perovskite cell was the application of $CH_3NH_3PbBr_3$ and $CH_3NH_3PbI_3$ as dye in dye-sensitized solar cells. The power conversion efficiency was obtained as 3-4 % with the usage of liquid Br/I based electrolyte in these cells (Kojima *et al*., 2009). However, the efficiency of the perovskite cells dramatically declined in very short time, since liquid electrolyte damaged the perovskite structure. In 2011, employing perovskite quantum dots method, the efficiency of perovskite solar cells became 6.5 % (Ye *et al*., 2016). A significant development was attained for perovskite solar cells by using a solid hole-transporting organic material called spiro-OMeTAD instead of liquid electrolyte in 2012. The power conversion efficiency of perovskite solar cells was increased about to 10 % (Kim *et al*., 2012). In early 2013, the application of poly-triarylamine (PTAA) as the hole-transporting material enhanced the efficiency up to 12 %. After the improvement of a new planar heterojunction in late 2013, the efficiency of the device reached to 15 % (Liu *et al*., 2013). In 2014, due to the applications of various kinds of spiro-OMeTAD as hole-transporting medium, the power conversion efficiency of perovskite solar cells was further increased to 16-17 %. The implementation of $FAPbI_3$-based perovskite solar cells created more efficient solar cells in 2015. A new form of perovskite was also fabricated using three different cations that were methylammonium, formamidinium, and cesium. This perovskite structure produced more stable perovskite solar cell and increased the efficiency to 21.1 % (Saliba *et al*., 2016).

The highest power conversion efficiency achieved was 21.2 % in 2017. Instead of mesoporous TiO_2, Lanthanum (La)-doped $BaSnO_3$ (LBSO) which is also a form of perovskite was used as an electron transport material. The new perovskite solar cell configuration contained methylammonium lead iodide layer and poly-triarylamine (PTAA)

as hole transport layer. LBSO supplied increased stability of perovskite solar cell under illumination which resulted in higher efficiency (Shin *et al*., 2017).

Perovskite solar cell technology researches expanded rapidly after observation of increased efficiency. In 2013, the perovskite solar cell was declared as the most important scientific development of the year 2013 by Science (342, December 2013) and Nature (504, December 2013) journals. And, the efficiency of the perovskite solar cells increased to 21.2 % in 2017 (Shin *et al*., 2017).

In this thesis, organolead halide perovskite solar cells will be investigated. The published articles about perovskite solar cells are mentioned in the Literature Survey (Chapter 2). The basis of perovskite solar cell structure and its working principles are explained in detail. In Chapter 3, the materials used in production of perovskite and the solar cell fabrication steps are presented. In Chapter 4 (Results and Discussion), results of the experiments are indicated and discussed. Finally, the main conclusions and recommendations are briefly expressed in Chapter 5.

2. LITERATURE SURVEY

2.1. Solar Cells

Solar cells are electrical devices, which can convert the solar energy into electricity by photovoltaic effect. Therefore, the first step of the photovoltaic invention can be considered as the observation of photovoltaic effect by Alexandre Edmond Becquerel in 1839 (Becquerel, 1839). Charles Fritts made the first solar cell consist of selenium with a thin layer of gold in 1883. However, selenium solar cells failed to convert enough sunlight into electricity. In 1954, the first efficient solar cells were invented in Bell Laboratories by Daryl Chapin, Calvin Fuller, and Gerald Pearson. These solar cells were silicon based solar cells with 8 % efficiency (Chapin *et al*., 1954).

The first famous application of the solar cells was on the Vanguard I satellite in 1958. Solar cells were added on the satellite body as an alternative energy source. In 1960s, solar cells became the major energy source of satellites with the increasing efficiency. The cost of solar cells was quite high to be used in the Earth; Elliot Berman designed less costly solar cells in early 1970s (Perlin, 1999).

In the early 1970s, the terrestrial applications of solar cells attracted attentions of companies to produce commercial products. The use of photovoltaics in telecommunication systems triggered the improvement of the cell technology. In addition, the first modern solar cells were fabricated in 1976. By the 1980s, manufacturers started to be interested in the cell production since it became a reliable field to invest. Recently, solar cells are part of a global energy industry competing with the other renewable technologies (Green, 2005).

Solar cell technologies are classified as three generations. The first generation solar cells are the traditional cells made from silicon. The silicon based photovoltaics dominate the market and they are currently most efficient solar cells. Single crystal silicon (c-Si) and multicrystalline silicon (mc-Si) are different applications of silicon technologies (Green, 2005).

The second generation solar cells are mainly amorphous silicon (a-Si), Cadmium telluride (CdTe) and Copper indium gallium diselenide (CIGS) technologies with 10-15% efficiency. They are called thin film solar cells due to their micrometers thickness. Since the second generation solar cells do not use silicon wafers and consume less, they can reduce the production cost. However, they are made from scarce elements, which is a limiting factor for commercial usage (Green, 2005; Giacomo *et al*., 2014).

The third generation involves some emerging technologies, which has been studied for 10 years; the third generation solar cells are mainly dye-sensitized solar cells, organic solar cells, quantum dot solar cells, polymer solar cells and perovskite solar cells (Tong *et al*., 2015; Shin *et al*., 2017). The object of these technologies is to have high performance with using cheap, non-toxic, and widely available materials (Bella, 2015). The studies have been resulted in considerable improvement in efficiency, stability and reproducibility in recent years (Snaith, 2013).

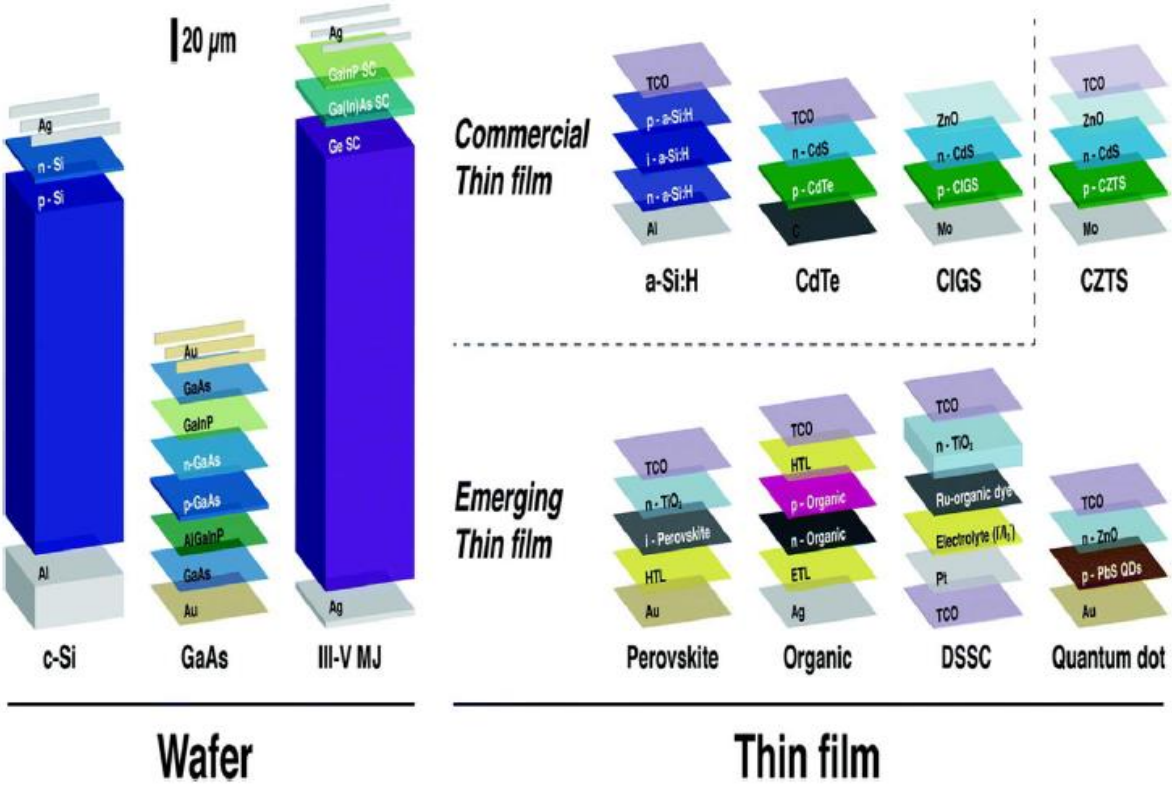

Figure 2.1. The diagram of solar cell designs for three generations (Mehmood *et al.*, 2017).

Especially perovskite solar cells have become quite popular in recent researches; due to their suitable properties, the power conversion efficiency of perovskite photovoltaics increased from 3.8% to 21.2% in a short time (Tong *et al*., 2015).

2.2. Perovskites

Perovskites were found by a German mineralogist Gustav Rose in 1839 as a mineral structure of calcium titanium oxide ($CaTiO_3$). Later, this mineral structure was defined by Russian mineralogist Lev Perovski and is named after Perovski (Chen *et al*., 2015).

Perovskite is a name for materials with the same chemical structure as ABX_3 where A and B are cations while X is an anion (Snaith, 2013; Chen *et al*., 2015). A is large cation with high electropositivity, while B is the smaller metal cation (Petrović *et al*., 2015). The larger cation A can be Cs, Ca, methylammonium, ethylammonium, and formamidinium while small cation, B is usually Pb^{2+}, Sn^{2+}, and Ge^{2+} (Mahmud *et al*, 2017). X represents oxide or halide anions as O^{2-} and I^-, Cl^-, and Br^- (Petrović *et al*., 2015). Figure 2.2 shows the cubic structure of perovskite representing cations and anion separately. B cation and X anion form an octahedral structure as BX_6 to become stable (Ubani *et al.*, 2017).

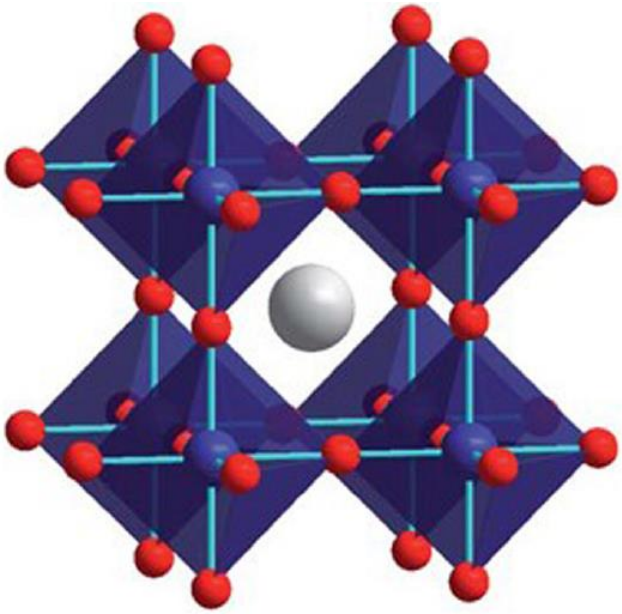

Figure 2.2. Perovskite structure ABX_3, where A is grey, B is red and X is blue spheres and octahedral structure formed by B and X as BX_6 (Petrović et al., 2015).

Perovskites can form multidimensional structures having the same chemical formula as it is displayed in Figure 2.2. Different combinations of various components can create this structure. Oxide-based perovskites were mostly studied because of their ferroelectric, magnetic and superconductive properties (Park *et al*., 2015).

In 1958, Moller discovered halide-based perovskite that was cesium lead halides ($CsPbX_3$). In 1978, Weber and Naturforsch used methylammonium as large cation of perovskite structure. Methylammonium is the first organic molecule applied as a cation in halide anion (I, Cl, Br) containing perovskites (Chen *et al*., 2015).

Perovskite solar cells mostly involve organometal halide perovskites which have methylammonium as an organic cation, 2+ charged inorganic cations such as Ge^{2+}, Pb^{2+}, Sn^{2+} and halide anions. The chemical content of perovskite affects its electronic structure and bandgap. Especially, halide ions lead to change in bandgap with the replacement of valance and conduction bands. The valance band changes with the halide ion used as I, Br or Cl, valance orbital becomes 5p, 4p or 3p. As a result, bandgap energy can be manipulated by the halide ion selection (Mehmood *et al.*, 2017).

On the other hand, the organic cation does not have a direct relationship with the bandgap. However, the cation can affect the electronic structure of perovskite causing change in bandgap. Therefore, the right choice of organic cation is crucial for conductivity of perovskites. Also, the large cation plays a critical role in formation of the perovskite structure which is related with the conduction properties of perovskite. As the dimensions of perovskite increases from non-dimensionality to 2D or 3D, the conductivity of the perovskite rises (Petrović *et al*., 2015; Mehmood *et al.*, 2017).

Perovskites are recently used as a key material to produce efficient solar cells. First application of perovskite was as a dye for dye-sensitized solar cells by Miyasaka *et al*. in 2009. Then, the photovoltaic researches focused on the advancement of the perovskite applications in solar cells (Tong *et al*., 2015).

2.3. Organolead Halide Perovskite Solar Cells

Organolead halide perovskite solar cells consist of perovskite material which is used as light absorber in the cell structure like a dye used in dye sensitized solar cells. Organolead halide solar cells draw the attention of researchers due to optical and electrical properties providing high efficiency and also because of being produced from abundant sources (Kojima *et al*., 2009).

The first usage of the organolead perovskite cell was the application of $CH_3NH_3PbBr_3$ and $CH_3NH_3PbI_3$ as dye in dye-sensitized solar cells by Miyasaka *et al*. in 2009. The achievement of high efficiency in organolead halide perovskite solar cells originated from the optoelectronic properties of the perovskite. These properties are high absorption coefficient, proper band gap, large charge mobilities, long diffusion lengths, long carrier lifetime, low-cost precursor materials, and simple solution processability. These characteristics have allowed the significant advancement of perovskite photovoltaics with efficiencies increasing from 3.8% to over 21.2 % in very short time (Kim *et al*., 2012; Xiao *et al.*, 2016; Bakr *et al*., 2017; Shin *et al*., 2017).

The strong absorption of organolead halide perovskite provides reduction in charge and energy loss during operation and less amount of absorber usage. Also, the absorption coefficient of organolead halide perovskite is higher than 3.0×10^4 cm^{-1} in visible light spectra. This means that the thickness of perovskite film should be in between 300 and 600 nm (Xiao *et al*., 2016).

The efficiency of perovskite solar cells has achieved the highest efficiency of commercial photovoltaics. The improvement of perovskite solar cells in 8 years is given in Figure 2.3. Also, the cost of perovskite solar cell production is much less than the conventional commercial products. The processing methods such as dip coating, spin coating, and screen printing provide low production cost which makes perovskite solar cells promising devices (Mehmood *et al*., 2017).

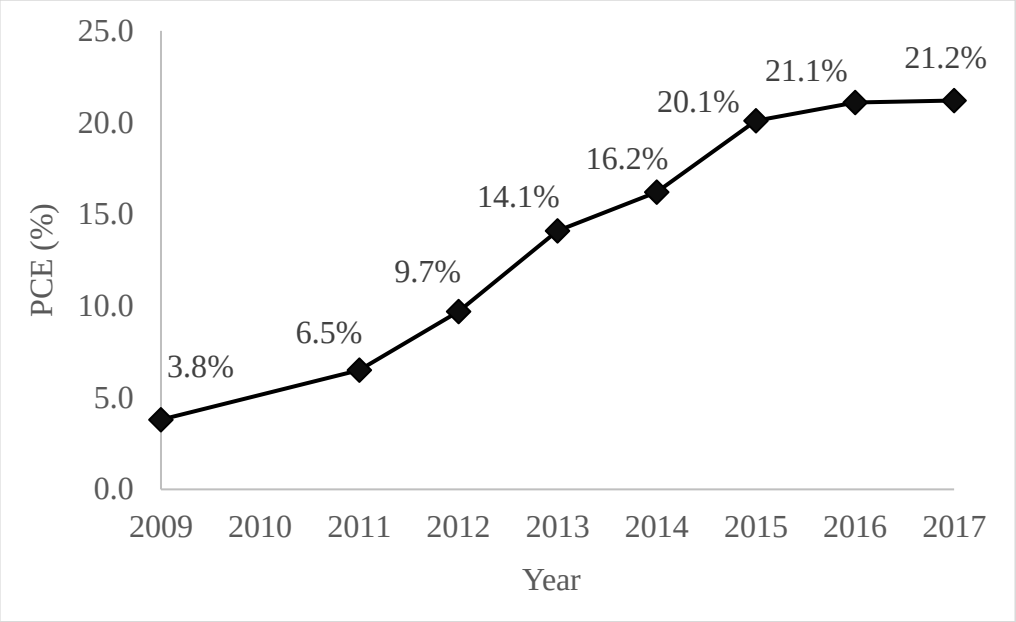

Figure 2.3. Power conversion efficiency improvement of perovskite solar cells in 2009-2017 (NREL, 2017).

The organolead halide perovskite solar cells were designed like dye sensitized solar cells. The perovskite layer is constrained by electron transport layer (ETL) and hole transport layer (HTL). In order to supply current along the cell, the metal electrode and an anode such as ITO or FTO substrates are added to the structure. This commonly used configuration with layers of materials is displayed in Figure 2.4. The structure of the perovskite solar cell can be manipulated by changing the positions of ETM and HTM or using various metal electrodes. In addition, the type of used ETM and HTM also alters the solar cells structure (Tong *et al*., 2015).

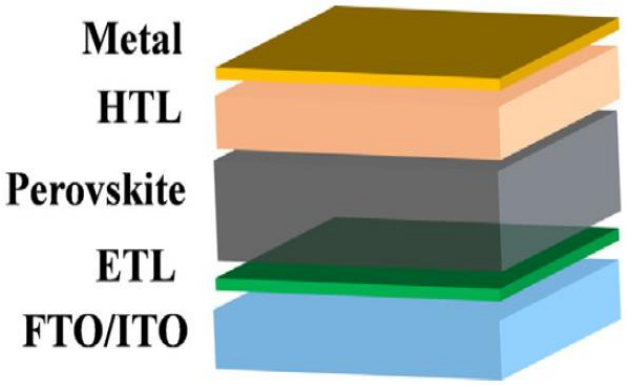

Figure 2.4. General perovskite solar cell configuration (Marinova *et al*., 2017).

A solar cell mechanism works under illumination. First, light is absorbed by the absorber material. The absorption of light leads an electron to higher energy levels. The electron with high energy state leaves the cell from an outer circuit. Then, the electron comes back to the cell filling the hole created. Perovskite solar cells have perovskite layer as light absorber who create the energetic electron and a hole. Electrons get higher energy on LUMO level, while holes are decreased to HOMO level. The charge carriers, electron and hole are extracted and transported by electron transport layer and hole transport layer, respectively. Hole is carried to metal electrode while electron moves to ITO/FTO substrate which acts as an anode. An outer circuit is linked to both electrodes, which leads electrons to return the cell filling the holes (Tong *et al*., 2015; Han *et al*., 2017; Marinova *et al*., 2017).

The performance of the perovskite cell depends on charge transport and extraction steps. The highest occupied molecular orbital (HOMO) of HTM should be higher than valance band maximum (VBM) of perovskite, which means that HTM is capable of high performance. Also, the conduction band minimum (CBM) of ETM should be lower than that of perovskite material, indicating the efficient ETM (Park, 2015; Tong *et al*., 2015).

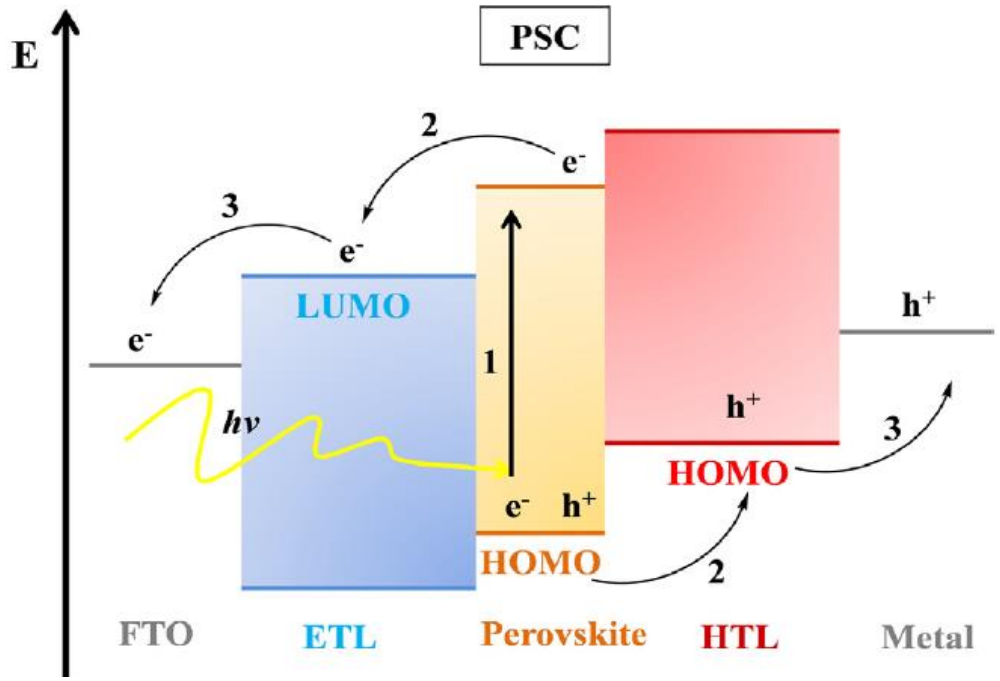

Figure 2.5. Perovskite solar cell working mechanism: 1-light absorption and charge generation, 2- charge transport, 3- charge extraction (Marinova *et al*., 2017).

2.4. Perovskite Solar Cell Architecture

Perovskite solar cells are fabricated based on perovskite layer enclosed by using layers of electron transport layer (ETL) and hole transport layer (HTL). The position of the charge transport layers determines the structure of perovskite solar cells. The solar cell is usually arranged as n-i-p (negative-intrinsic-positive) which represents ETL-Perovskite-HTL order. In contrast, p-i-n (positive-intrinsic-negative) indicating HTL-Perovskite-ETL order is another cell configuration. Also, the choice of material type applied on the bottom transparent electrode makes the structure mesoporous or planar. Overall, there are two main device architectures: mesoporous and planar. Figure 2.6 shows a representative picture of mesoporous and planar junction (Marinova *et al*., 2017; Mehmood *et al*., 2017).

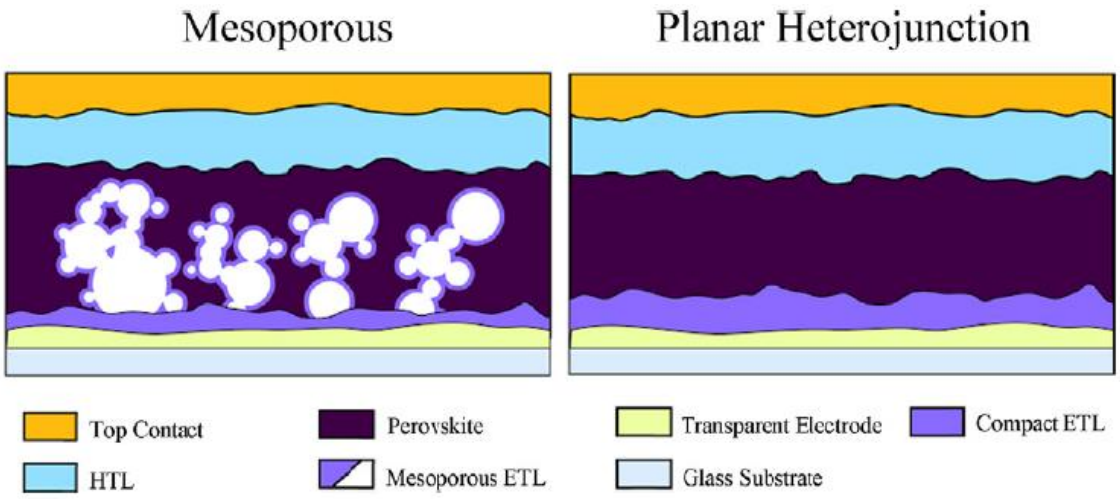

Figure 2.6. Perovskite solar cell configurations (Chen *et al*., 2015).

2.4.1. Mesoporous Architecture

Mesoporous perovskite solar cell configuration has a metal oxide electron transport layer with an extra compact layer covered on the transparent electrode. The most common architecture includes TiO_2 as compact layer and mesoporous layer. The solar cell structure is generated by using FTO substrate which is coated by compact and mesoporous TiO_2, respectively. Then, perovskite is deposited on the mesoporous layer. Afterwards, HTM is coated on the perovskite layer (Luo *et al.*, 2016).

The possibility of electron and hole charges to combine with each other is much higher in mesoporous configuration. Therefore, charge transport and extraction decreases due to recombination of charges which causes declined efficiency of mesoporous perovskite solar cells. Although a significant property of perovskite was its long diffusion length, mesoporous structure of ETL causes diminishing in length of diffusion. In order to prevent recombination of charges, nanomaterials such as ZnO nanorods and 3D-TiO_2 nanoparticles can be used instead of mp-TiO_2. In addition, the surface of mesoporous material which is in contact with perovskite can be modified. For instance, ultrathin MgO nanolayer can be applied to the interface between mp-TiO_2 and perovskite material (Mehmood *et al*., 2017).

Zinc oxide is essentially an alternative material to TiO_2 with mesoporous configuration. ZnO layer consists of nanorods, which gives higher efficiency with methylammonium iodide perovskite solar cells. However, there is also recombination problem in ZnO scaffolds. Since mesoporous configuration makes the solar cell structure much more complicated, this configuration is hard to implement with a high performance (Chen *et al*., 2015; Hatamvand *et al*., 2017).

2.4.2. Planar Architecture

Planar heterojunction is a configuration in which perovskite material stays between electron transport layer without mesoporous scaffold and hole transport material. The planar configuration is not complicated as the mesoporous architecture. Also, in contrast to mesoporous device production processes, planar devices are fabricated at relatively low temperatures. It is easy to produce with proper film formation methods. Since the planar device supplies a smooth pattern, the device structure formation and material's electrical characteristics are much important issues. The performance of the cell depends on both the material and the fabrication method of perovskite solar cells. The continuous film formation during processing is significant to prevent the pinholes on the surfaces (Salim *et al*., 2015; Mehmood *et al*., 2017).

The planar configuration is a simply generated structure. Therefore, in order to improve the planar type solar cells usage of proper HTL and ETL materials, enhancement in the interface behavior of HTL and ETL, and thin film fabrications methods are studied in

detailed manner. Since the fabrication of planar devices is not complicated, it is possible to generate the planar type perovskite solar cells for commercial purposes with low production cost. The perovskite layer of planar heterojunction has higher performance compared with mesoporous configuration regarding electron and hole carrier mobility (Tseng *et al.*, 2015; Chen *et al*., 2015).

The planar solar cell structure is classified into two groups which are n-i-p and p-i-n type configurations. The classification represents the deposition order of ETL and HTL layers on conductive glass substrate.

2.4.2.1. n-i-p Type Planar Solar Cells. The most common planar architecture is n-i-p type whose configuration is arranged as ETL is applied on transparent conductive layer. And then perovskite material is deposited on ETL. Afterwards, HTL is the top layer of the solar cell structure which is completed with a metal contact. The incident light first comes to ETL layer passing through the conductive layer creating electron-hole pairs. Planar configuration with n-i-p arrangement has higher efficiency than that of mesoporous architecture (Chen *et al*., 2015, Salim *et al*., 2015; Mehmood *et al*., 2017).

TiO_2 can be also employed as ETL for planar n-i-p type configuration. The production method of TiO_2 makes its structure either mesoporous or planar. The low temperature processing of TiO_2 via sol-gel method results in planar properties of nanoparticles. Yella *et al*. studied a low temperature processed TiO_2 as ETL in the production of TiO_2/Perovskite/Spiro-OMeTAD planar solar cell with 13.7 % power conversion efficiency (Yella *et al*., 2014). In addition, a n-type metal oxide ZnO which is generated by low-temperature process was used as ETL of planar perovskite solar cells giving 15.7 % efficiency (Liu and Kelly, 2014).

2.4.2.2. p-i-n Type Planar Solar Cells. The inverted planar configuration is p-i-n type which is exactly opposite of n-i-p type devices. Here, after transparent conductive layer, HTL is deposited. The bottom of the perovskite becomes HTL while upper layer is ETL. The light enters from the transparent conductor passing through HTL. The first application of p-i-n type solar cells was designed using PEDOT:PSS as p-type material and PCBM as n-type material (Salim *et al*., 2015).

You et al. studied p-i-n structure using p-type NiO (HTM) and n-type ZnO (ETL). Perovskite was deposited on NiO layer with sequential deposition method. The efficiency of perovskite solar cell was 16.1 % which is as high as conventional n-i-p type structured solar cells (You *et al.*, 2015).

Ciro *et al.* fabricated p-i-n type planar perovskite solar cells with NiO hole transport material and PCBM electron transport material under ambient air with high humidity applying temperatures lower than 100℃. This structure resulted as 11.1 % power conversion efficiency reducing hysteresis (Ciro *et al.*, 2017).

2.4.3. HTM-free and ETM-free Configurations

Hole and electron transport materials are employed to extract the charge carriers. However, solar cells can be produced without containing charge transport layers. HTM-free and ETM-free devices are fabricated to minimize the production cost of solar cells. The lessening of a material is a gain for mass production purposes (Chen *et al*., 2015; Cohen *et al.*, 2015).

HTM-free structure is a practicable option for perovskite solar cells owing to hole transporting characteristics of perovskite material. The HTM-free solar cells have relatively low performance in terms of their open circuit voltage and fill factor (FF) values. According to the results, HTM-free solar cells are still in beginning stage of progress. Since the electron and hole charges are easily recombined due to absence of HTM in the structure, HTM-free solar cells are not highly efficient. The performance of HTM-free perovskite solar cells can be enhanced by morphological and structural control which prevents recombination of charges and improves charge collection. Etgar *et al.* first achieved 5.5% efficiency on Perovskite/TiO_2 structure without HTM. Moreover, Shi *et al.* fabricated TiO_2/Perovskite/Au structured solar cell using 2-step deposition of perovskite reaching 10.49% power conversion efficiency (Cohen *et al.*, 2015, Tong *et al*., 2015; Wei *et al.*, 2016).

ETM-free structure is another employed configuration in production of perovskite solar cells. On the other hand, solar cells without ETM achieved high performance in comparison with the conventional structure. Due to high hole extraction by HTL, the absence

of ETM does not largely effect the performance of the cell. Also, because of high hole transport, the perovskite lacks hole carrier preventing the recombination of charges (Chen *et al*., 2015; Gamliel *et al.*, 2015).

Liu *et al.* fabricated ETL-free solar cells comparing with the solar cells that have ZnO as ETL. The structure of the cell is dependent on Ag/HTM/Perovskite/ITO configuration which achieved 13.5% efficiency. This result shows that ETM is not necessary to obtain high performance of perovskite solar cells (Liu *et al.*, 2014).

2.5. Morphology of Perovskite Film

The performance of perovskite solar cells depends on the perovskite formation along the cell. The perovskite film quality should be high to provide efficient perovskite solar cells with high open circuit voltage and current density. The highly efficient perovskite solar cells require crystallization with high surface coverage, reduced pin holes and good morphology. The crystallization process is related with the perovskite deposition method, stoichiometry of components, solution processing methods, additives, and thermal treatment during the fabrication of perovskite film (Chen *et al.*, 2015; Salim *et al.*, 2015).

2.5.1. Perovskite Deposition Methods

The methylammonium lead iodide perovskite is formed on charge transport materials to obtain an efficient absorbent layer by either single step deposition method or sequential deposition method. Both procedures were employed in various studies to generate continuous perovskite film as mentioned in the following sections.

2.5.1.1. One-Step Deposition. In this method, lead iodide and methylammonium iodide are mixed in an organic solution such as DMF, DMSO or GBL and casted on glass substrate coated with charge transport layer either ETL or HTL. After spin coating process, the glass substrates are annealed at various temperatures to form perovskite layer with continuous coverage (Mehmood *et al.*, 2017).

The first perovskite solar cells were mostly fabricated by single step perovskite deposition method resulting inefficient solar cells. Since the crystal formation cannot be properly controlled in this method, film coverage and crystal grains becomes weak causing poor performance of solar cells. Even one-step deposition method has low cost and easy application, efficiency of the solar cell is limited due to insufficient surface coverage causing pin holes. The electrical performance of perovskite solar cells is directly related with the film coverage of perovskite. The crystallization occurs immediately after spin coating the precursor solution because of rapid solvent removal and strong ionic interactions (Salim *et al.*, 2015; Yang *et al.*, 2016; Mehmood *et al.*, 2017).

Stranks *et al.* produced perovskite layer via single step deposition under nitrogen environment which is followed by annealing at 90 ℃. Due to nitrogen atmosphere and low annealing temperature, a continuous perovskite film was obtained with 12% efficiency. Although the solar cell has high performance, perovskite was not evenly distributed on the surface which creates an adverse effect (Stranks *et al.*, 2015).

In order to improve the surface coverage in planar devices, precursor molar ratio is changed to 1:3 PbI_2:MAI (Lee *et al.*, 2012). The change in the molar ratio increased the performance of the solar cell. The same method is further developed by Zhou *et al*. achieving 19% power conversion efficiency (Zhou *et al*., 2014). In addition to the molar ratio, lead halide component is altered to have better film morphology through the solar cell (Chen *et al.*, 2015; Salim *et al.*, 2015; Xiao *et al.*, 2016; Mehmood *et al.*, 2017).

2.5.1.2. Two-Step Deposition. Sequential deposition of perovskite provides an easily controllable crystallization which leads a smooth perovskite coverage reducing pin holes and achieving high performance. In this method, lead iodide and MAI are dissolved in DMF and 2-propanol separately. Then, PbI_2 and MAI are coated on metal oxide coated substrates respectively (Xiao *et al.*, 2016; Lui *et al.*, 2017).

Burschka *et al.* tried the two-step deposition method to cover a metal oxide layer with perovskite for the first time. It was observed that single deposition suffers from uneven film formation causing weak performance. Therefore, in order to control the crystal formation properly, sequential deposition was applied. The TiO_2 coated glass was covered with PbI_2

by spin coating and then annealed. The lead iodide film was dipped into MAI solution of in 2-propanol. This method increased the power conversion efficiency of perovskite solar cell to 15% (Burschka *et al.*, 2013).

In addition to mesoporous device, two-step deposition was employed in planar solar cells. However, completion of the conversion from MAI and PbI_2 to $MAPbI_3$ takes longer time since MAI should spread into the PbI_2 layer to start the reaction. Therefore, crystal formation of perovskite becomes easy to manipulate. Also, annealing after MAI casting supplies both fast removal of solvents and high power conversion efficiency (Burschka *et al.*, 2013; Salim *et al.*, 2015).

Chiang *et al.*, applied spin coating of PbI_2 and MAI precursors with a very slow speed. Due to slow spinning, solvents evaporated slowly. Therefore, MAI could penetrate PbI_2 layer without additional heating. Overall, annealing was eliminated by manipulating the spin speed. The fabricated planar solar cell demonstrated 16.3 % efficiency (Chiang *et al.*, 2014, Salim *et al.*, 2015).

You *et al.* used two-step deposition method to coat NiO hole transport layer with perovskite. Since quality of perovskite synthesized by one-step deposition method is very poor because of rough surface of NiO, sequential deposition was employed achieving 16.1 % PCE. Both PbI_2 and MAI solutions were deposited by spin coating. Then, the resulting perovskite layer was annealed to complete the conversion (You *et al.*, 2015).

2.5.2. Precursor Composition

The molar ratio of precursors is one of the factors that influences the perovskite film quality. The proper composition varies according to the halide type of the organolead halide perovskite. The molar ratio of MAI to PbI_2 which gives high efficiency is 1:1, while the ratio of $PbCl_2$ to MAI has better film quality with 1:3 (Chang *et al.*, 2016). The equimolar solution results in irregular surface of perovskite film with microfiber occurrence due to high content of PbI_2. Therefore, decreased amount of PbI_2 yields decline in microfiber and pin hole formation, descending the precursor ratio. High quality perovskite film is obtained by the reduction of PbI_2 (Chang *et al.*, 2016). However, the balance in the precursor composition

is significant because high molar ratio may cause unreacted MAI while low molar ratio leads excessive PbI_2 within the perovskite layer. The unreacted species cause drop in the device performances. In addition, the proper ratio differs for perovskite layers with different thicknesses (Chen *et al.*, 2015; Salim *et al.*, 2015; Mehmood *et al.*, 2017).

2.5.3. Solvent Engineering

The solvent selection is one of the most substantial parameter that affects the perovskite film formation and quality. Perovskite is synthesized via mostly PbI_2 and MAI which have separate chemical properties. Therefore, the solvent which is proper for both precursors has limited options. DMF, DMSO and GBL are the most widely used solvents which facilitate the crystallization of perovskite. These solvents are chosen in terms of their solubility, viscosity, and boiling point properties that are effective in quality of film formation (Chen *et al.*, 2015).

DMF was employed as solvent of perovskite precursor solution for the first time by Snaith *et al.* in order to create perovskite layer on Al_2O_3 scaffold. DMF forms a complex with lead halide component during the film generation resulting improved performance of perovskite absorber. Afterwards, DMF was also used as solvent in planar devices (Snaith *et al.*, 2013).

GBL is also deposited on mesoporous layer of ETL, providing enhanced light absorption of perovskite. When it is compared to DMF, DMF has lower boiling point than GBL which supplies relatively high growth rate of $MAPbI_3$. Due to high rate of formation, surface of perovskite becomes uneven with pin holes and insufficient crystallization (Chen *et al.*, 2015).

Moreover, mixture of the widely used solvents results in improved crystallinity of perovskite film. A small amount of GBL addition to DMF causes crystals with small grain sizes. Because the boiling point of mixture is increased, perovskite growth rate is declined preventing the microfiber generation due to unreacted PbI_2. A similar mixture with DMSO and GBL produces increased performance of perovskite absorber (Chen *et al.*, 2015; Mehmood *et al.*, 2017).

In addition, the solvents are removed while spin coating process and thermal heating. In order to accelerate the evaporation of excess solvents, non-dissolving materials are dropped on the perovskite film while spinning. Toluene and chlorobenzene are mostly implemented to fasten the crystallization of perovskite layer. First, a transparent layer is formed and then, color becomes black with the formation of perovskite. This method provides uniform distribution of perovskite material along the solar cell (Chen *et al.*, 2015; Salim *et al.*, 2015; Xiao *et al.*, 2016; Mehmood *et al.*, 2017).

2.5.4. Solution Processing Techniques

The fabrication method of perovskite solar cells influences the performance of the device. Solution processing is a good alternative to perovskite synthesis, due to its solubility properties. Good solubility of perovskite provides usage of low cost and easy techniques such as spin coating, dip coating, spray coating, and screen printing. Also, there are other options to produce perovskite such as drop casting and thermal evaporation (Petrović *et al.*, 2015; Asghar *et al*., 2017).

Spray coating is a low-cost method with rapid perovskite deposition, but this method leads inefficient perovskite film. In addition, screen printing method wastes too much material while perovskite depositing, which is not suitable for further improvements. Moreover, even drop casting is not a proper technique to be used in laboratory scale, it is efficient way to synthesize perovskite. One drawback of drop casting is the difficulty in control of the film thickness. Thermal evaporation is another way to fabricate perovskite solar cells, which is used for metal deposition. This method is usually used for back electrode deposition (Krebs *et al.*, 2009; Asghar *et al*., 2017).

2.5.4.1. Spin Coating. The most widely used method is spin coating due to its simplicity in applications. Spin coating method contains perovskite deposition on a conductive substrate and spinning of the substrate. Through spin coating, film thickness of the perovskite can be controlled easily by manipulating the solution concentration and viscosity and by changing the spin speed of the device. Spin coating is advantageous due to its low cost, need for small amount of solution to cover substrate surface, and ability to create multilayer on a substrate (Krebs *et al.*, 2009; Petrović *et al.*, 2015; Asghar *et al*., 2017).

2.5.4.2. Dip Coating. Dip coating is another common method to produce perovskite solar cell. It comprises of dipping a substrate in the coating solution forming desired film. This method can be applied in two ways to produce perovskite layer. It can be used as one-step deposition of perovskite employing PbI_2-MAI solution. The substrate is dipped into the solution to form perovskite film and waited for required time to obtain desired thickness. On the other hand, dip coating can be a part of two step deposition method. First, lead iodide is coated on a substrate with spin coating which is followed by dipping PbI_2 layer into MAI solution. The perovskite film is formed inside the solution. Also, post treatment which is thermal annealing may be necessary to obtain complete conversion (Petrović *et al.*, 2015; Huang *et al.*, 2016).

2.5.5. Annealing

Annealing is performed to trigger the reaction between the precursor materials and to speed up this reaction. Thermal annealing process provides better perovskite formation with an advanced crystallization and grain development. Also, heat treatment is employed to discard excess precursor materials and by-products (Salim *et al*., 2015; Xiao *et al*., 2016; Mehmood *et al*., 2017).

Temperature of annealing and annealing time are factors that influence the perovskite film quality. An increase in either time or temperature of the annealing causes poor surface coverage of perovskite. High temperature annealing which is applied at greater than 100℃ causes islands in perovskite film. Also, the amount of PbI_2 is increased due to evaporation of MAI (Eperon *et al*., 2014).

Annealing at low temperatures, mostly less than 80℃, results in insufficient film formation. Even the annealing time is extended, the perovskite formation is not completed with an adequate coverage. Due to poor crystallinity and weak film formation, absorption of perovskite layer becomes poor. Therefore, low performance of the perovskite solar cells is observed. Thus, the annealing process should be elaborately adjusted considering both the temperature and the duration of heating (Chen *et al.*, 2015; Mehmood *et al.*, 2017).

Flash annealing is also a method for annealing process. This method requires fast heating to a high temperature and heating for short time. During application of heat, the perovskite structure is formed. Saliba et al. expressed that flash heating is useful for planar devices while mesoscopic cells have inadequate performance with flash heating. (Salim *et al.*, 2015; Saliba *et al*., 2016).

2.6. Hole Transport Materials (HTMs)

Perovskite which is light absorber material produces charges that should be collected and transported to create current along the solar cell. The holes that are created in perovskite film are extracted by hole transporting materials. HTM is a material that plays a significant role in photovoltaic performance of perovskite solar cells. In order to fabricate efficient solar cells, HTMs should meet several requirements. HTM should have high hole mobility to prevent charge losses and recombination. The HOMO level of HTM should conform with that of perovskite material. HTMs should be highly stable under environmental conditions. It should be thermally stable and should not degrade under humidity and oxygen exposure. Also, hole transport materials should have low cost for the future applications (Bakr *et al.*, 2017).

HTMs which are used in perovskite solar cell fabrications can be classified in two main groups as organic and inorganic HTMs. Organic HTMs involves small molecules and polymers in terms of their structure. HTMs with small molecules includes spiro-OMeTAD, pyrene derivatives, and thiophene derivatives. In addition, P3HT, PTAA, and PEDOT:PSS are the examples of polymer HTMs. Inorganics, mostly metal oxides that are used as hole transport material are CuI, CuSCN, NiO, GO, and Cu_2O (Tong *et al*., 2015; Xiao *et al*., 2016).

2.6.1. Organic HTMs

2.6.1.1. Spiro-OMeTAD. 2,2′,7,7′-Tetrakis(N,N-diphenylamino)-9,9-spirobifluorene which is called spiro-OMeTAD is the most widely used HTM in perovskite solar cell studies. It was first utilized as HTM in 2012 by Kim *et al.* achieving 9.7% power conversion efficiency (Kim *et al.*, 2012). Since then, spiro-OMeTAD has frequently employed as HTM for both

planar and mesoporous perovskite solar cells. However, spiro-OMeTAD possesses low hole mobility and weak conductivity due to its particular structure. Therefore, chemical doping is implemented to increase its charge transport ability. Addition of lithium bis(trifluoromethylsulphonyl) imide (Li-TFSI), 4-tertbutylpyridine (TBP), and cobalt dopants prevent the charge recombination enhancing the charge mobility. Also, these additives provide better contact between HTM and perovskite surface (Chen *et al*., 2015; Tong *et al*., 2015; Xiao *et al*., 2016; Bakr *et al*., 2017).

2.6.2. Inorganic HTMs

2.6.2.1. NiO. NiO is the first metal oxide which was used as HTM in perovskite solar cells. There are both mesoporous and planar applications of p-type NiO depending on its generation method. Due to its large band gap, high hole mobility and valance band level meeting the perovskites properties, NiO became popular as an inorganic HTM in perovskite solar cell fabrication studies (Tong *et al*., 2015; Zhang *et al*., 2015; Bakr *et al*., 2017).

Docampo *et al.* used NiO as HTM for the first time with mixed halide perovskite material. However, because of insufficient surface coverage of perovskite layer, HTL was in contact with ETL. This triggered the recombination of charges reducing device efficiency to 0.1% (Docampo *et al.*, 2013).

Tian *et al.* produced mesoporous NiO layer to be used as HTM of perovskite solar cell device with PCBM as ETL by keeping the thickness of NiO compact and mesoporous layers at a certain level, which resulted in 1.5% increase in the device efficiency (Tian *et al.*, 2014). Furthermore, Zhu *et al.* fabricated inverted mesoporous perovskite solar cells with NiO nanocrystal HTM achieving 9.1 % power conversion efficiency (Zhu *et al.*, 2014). On the other hand, You *et al.* generated inverted planar configuration of perovskite solar cell using NiO as HTM yielding 16.1 % power conversion efficiency with high quality perovskite film coverage (You *et al.*, 2015). In addition, Cu-doped NiO was produced to apply as a HTM in inverted planar solar cells. Jung *et al.* reported solution-processed Cu doped NiO at low temperatures leading thin films with smooth surface yielding 17.74 % PCE (Jung *et al.*, 2015; Ciro *et al.*, 2017).

2.7. Electron Transport Materials (ETMs)

Electron transport material is another charge carrier layer used in perovskite solar cells besides hole transport material. The electron charges are generated in light absorber perovskite layer needed to be collected and transported to prevent electron-hole recombination by ETM. Therefore, ETM has a direct influence on the device efficiency.

ETMs should have several characteristics to fabricate high performance perovskite solar cells. ETMs should be stable under ambient air conditions, durable under humidity. Also, ETMs should be cost efficient for large scale applications. Electron transport materials contain a wide range of organic and inorganic materials.

2.7.1. Organic ETMs

2.7.1.1. PCBM. [6,6]-Phelnyl-C-butyric acid methyl ester is an organic compound which is widely used as ETL in perovskite solar cells with high efficiency. It properly correlates with perovskite surface. PCBM has several derivatives in terms of its C component. C_{60}, C_{61} or C_{71} can be used in PCBM structure effecting the performance of the ETL (Jeng *et al.*, 2013; Chen *et al.*, 2017).

2.7.2. Inorganic ETMs

2.7.2.1. TiO_2. TiO_2 is the most common electron transport material used in perovskite solar cells. Both mesoporous and planar TiO_2 is applied as ETL. There are several production techniques to enhance electron extraction. TiO_2 is deposited on transparent conductive material by either spray pyrolysis or spin coating. Then, $TiCl_4$ was applied and annealed at high temperatures. Because high temperature annealing is an undesired implementation, sol-gel method was improved to synthesize TiO_2 (Chen *et al.*, 2015).

Qiu *et al.* produced TiO_2 nanowires to be used as ETM in perovskite solar cells, and observed that dense and small sized TiO_2 could be used in high performance devices (Qiu *et al.*, 2013). Also, Yella *et al.* used a new deposition method to produce TiO_2 nanoparticle enhancing the surface area, which resulted in perovskite solar cell with 13.7% PCE (Yella

et al., 2014). In addition, TiO_2 nanoparticles with addition of graphene was generated by Wang *et al.* achieving 15.9 % efficiency (Wang *et al.*, 2014).

2.7.2.2. ZnO. ZnO is a n-type metal oxide which is used as ETM in planar devices. ZnO thickness does not affect the solar cell performance because it is highly conductive material independent of the layer thickness. ZnO nanoparticles can be produced by various methods by annealing at relatively low temperatures (Chen *et al.*, 2015; Tong *et al.*, 2015; Xiao *et al.*, 2016).

Liu *et al.* generated ZnO nanoparticles as a thin layer by spin coating at room temperature. Instability of perovskite solar cell stems from the high temperature treatment is overcame by ZnO nanoparticle applications. Perovskite solar cell efficiency is increased to 15% (Liu *et al.*, 2014).

ZnO was used as ETL of inverted planar perovskite solar cells. You *et al.* covered perovskite layer which was deposited by sequential method with ZnO nanoparticles. The solar cell contained NiO as HTL. This structure reached to 16.1% power conversion efficiency (You *et al.*, 2015).

Hatamvand *et al.* investigated HTM free perovskite solar cells containing ZnO electron transport layer synthesized at low temperatures. The influence of ZnO nanoparticle concentration and ZnO thickness on the solar cell was studied. However, very low PCE was obtained due to the processing methods and temperatures (Hatamvand *et al.*, 2017).

3. EXPERIMENTAL SECTION

3.1. Materials and Equipment

CH_3NH_3I and PbI_2 are the main materials to synthesize perovskite. In addition, ITO coated glass, FTO coated glass with TiO_2 layer, and highly conductive hole and electron transport materials such as PCBM, ZnO, an ionic liquid (1-Ethyl-3-methylimidazolium bis (trifluoromethylsulfonyl)imide), and NiO which was produced from Nickel Acetate Tetrahydrate were used in order to fabricate perovskite solar cells. Also, Al and Cu tapes were implemented as the back electrode of the cells. DMF, 2-propanol, chlorobenzene and ethanol were the required solvents during experiments.

3.1.1. Materials

3.1.1.1. CH_3NH_3I (Methylammonium Iodide). Methylammonium iodide which is the main element of perovskite production, was purchased from Solaronix as a white powder. It is precursor material for metal-halide perovskites.

3.1.1.2. PbI_2 (Lead Iodide). Lead Iodide was purchased from Aldrich in powder form. It was used to produce perovskite material applying two distinct deposition methods.

3.1.1.3. Nickel Acetate Tetrahydrate. Nickel Acetate Tetrahydrate that was bought from Sigma-Aldrich was used to produce NiO solution. Nickel Acetate Tetrahydrate is in powder form with more than 99% purity.

3.1.1.4. ZnO (Zinc Oxide). Zinc oxide was purchased from Sigma-Aldrich to be used as electron transport material in p-i-n type perovskite solar cell design. ZnO nanoparticle size is less than 110 nm which is dispersed in butyl acetate with 40 wt%.

3.1.1.5. ITO (Indium Tin Oxide) Glass. ITO glasses were purchased from Sigma-Aldrich to be used as anode of the solar cells. ITO coated glasses have 8-12 Ω/sq surface resistivity and 25mm × 25 mm × 1 mm dimensions.

3.1.1.6. FTO (Fluorine Doped Tin Oxide) Glass Coated with TiO2. FTO glass slides coated with TiO_2 was bought from Solaronix. The scaffolding titania electrodes with 600 nm thick etched layer provides easy deposition of perovskite on the glass substrates.

3.1.1.7. Ionic Liquid (1-Ethyl-3-methylimidazolium bis (trifluoromethylsulfonyl) imide). The ionic liquid was used as electron transport material fabricating the perovskite solar cells. It was bought from Aldrich with high purity more than 98%.

3.1.1.8. PCBM. PCBM which is [6,6]-Phenyl C_{61} butyric acid methyl ester was applied as top layer material in TiO_2 based solar cells. It was purchased from Aldrich. PCBM is a n-type semiconductor with 6.1 eV HOMO and 3.7 eV LUMO.

3.1.1.9. Al Tape. Aluminum tape was purchased from Ted Pella, Inc. Al tape was used as back electrode of solar cells since it is an electrically conductive material. The tape comprises of aluminum foil and a conductive acrylic adhesive with 0.081 mm thickness, 12.7 mm width and 16.4 m length. Al tape is effective in conducting electricity and heat.

3.1.1.10. Cu Tape. Copper tape, which is defined as copper foil with nickel with conductive adhesive, was purchased from Ted Pella, Inc. Cu tape was utilized as back electrode of perovskite solar cells because it is an electrically and also thermally conductive material. The tape has 0.075 mm thickness, 8 mm width and 20 m length.

3.1.1. Equipment

The equipment used in this study is listed in Table 3.1.

Table 3.1. Equipment.

Equipment Name	Source
Spin Coater	Laurell
Source Meter	Keithley 2401
Solar Simulator	ABET Technologies
Sputter Coater	POLARON SC7640

3.2. Fabrication of Perovskite Solar Cells

The experiments were carried out generating two distinct perovskite solar cell structures. One of the solar cells was produced by using FTO coated glass with TiO_2 layer where TiO_2 acts as the electron transport layer. This solar cell had n-i-p (negative-intrinsic-positive) type design. Whereas, the other cell was a p-i-n (positive-intrinsic-negative) type solar cell that used NiO as a hole transport material. The structure of solar cells was designed based on their TiO_2 and NiO layers. Perovskite was deposited on TiO_2 and NiO coatings. The back electrode and the top layer of the cells were changed to observe their effects on the performance of the perovskite solar cells.

The solar cells with TiO_2 electron transport layer were fabricated by using FTO as anode which was coated with TiO_2. Perovskite was deposited on the TiO_2 layer. In order to provide electron movement, PCBM and ZnO were coated on perovskite as top layer. Both Al and Cu tapes were used as back electrode to complete the solar cell. These cells were designed to obtain planar n-i-p type structure. The fabricated cells were categorized in terms of their hole transport materials and perovskite deposition methods.

On the other hand, NiO hole transport layer on ITO coated glass was the basic unit of p-i-n type solar cells produced during experiments. After perovskite layer, ZnO or ionic liquid was implemented as electron transport layer. In addition, solar cells without electron transport material were fabricated due to easy electron movement through crystal structure of perovskite. The generated solar cells were classified with respect to the electron transport layers, perovskite deposition methods and the thickness of NiO layers.

3.2.1. Solar Cells with TiO_2 as ETL and PCBM as HTL

The solar cell structure with TiO_2 as electron transport layer and PCBM as top layer included perovskite layer in between ETL and HTL. TiO_2 was coated on FTO glass substrate. After the PCBM deposition, Al and Cu back electrodes were attached to the surface of the solar cell. Figure 3.1 shows the cell design. Procedure will be explained in detail in the following.

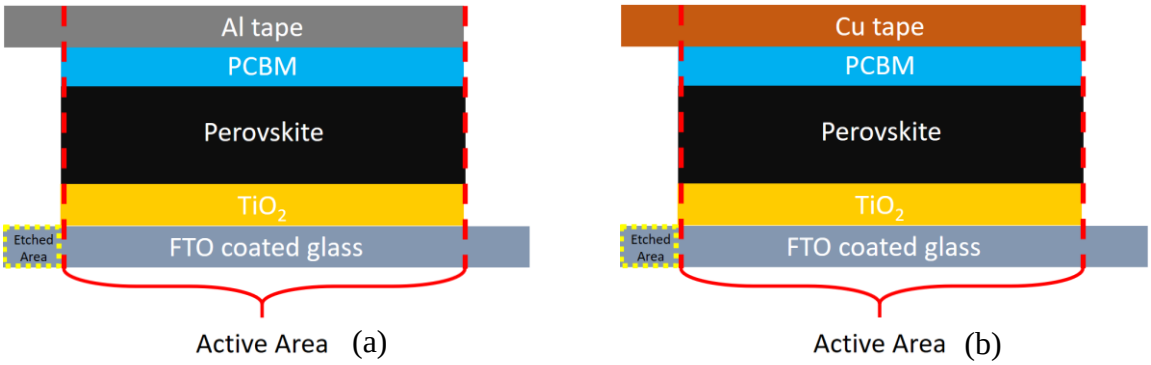

Figure 3.1. TiO_2 as ETL and PCBM as HTL solar cell structure with (a) Al tape back electrode, (b) Cu tape back electrode.

3.2.1.1. Cleaning of FTO and TiO_2 Coated Glass Substrates. FTO coated glass should have uncoated areas to prevent short circuit in solar cell. Therefore, some of FTO should be etched from the surface. However, the FTO glass substrate was already etched. Also, TiO_2 was coated on the FTO. Before perovskite deposition process, the substrate was washed with distillate water and ethanol to remove any dust from the surface of the glass. Figure 3.2 shows the details of the FTO coated glass substrate, etched and TiO_2 coated areas.

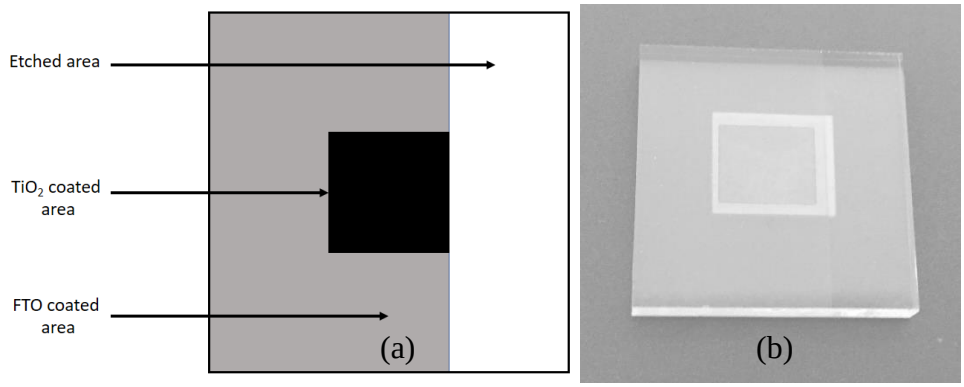

Figure 3.2. FTO and TiO_2 coated glass substrates (a) shows schematic representation of coated and etched areas, (b) shows glass substrate.

3.2.1.2. Perovskite Synthesis via 1-step Deposition Method. Perovskite which has molecular formula as $CH_3NH_3PbI_3$ was produced by using PbI_2 (Lead iodide) and CH_3NH_3I (Methylamonium iodide). One step deposition of perovskite involves dissolution of PbI_2 and CH_3NH_3I in DMF. The mixture was prepared by taking the molar ratio of CH_3NH_3I: PbI_2 as 3:1 and adding them into adequate amount of DMF. The mixture formed was stirred for 3 hours at 70℃ by the help of magnetic stirrer.

The resulting solution that had homogenous yellow view was coated on TiO_2 layer by spin coating in ambient air. The spin coating of perovskite precursor was applied with a speed of 2500 rpm for 20 s. Immediately after spin coating process, the substrate was put on a hot plate. The perovskite was annealed at 90℃ for 2 hours to form stabile perovskite crystals at the surface. The color of perovskite layer changed from yellow to brown or black in just several seconds after placing the substrate on the hot plate indicating that perovskite is properly formed.

Figure 3.3. Spin coating of perovskite.

3.2.1.3. PCBM Deposition. PCBM was dissolved in chlorobenzene with concentration of 50 mg/ml. The PCBM solution was stirred for 3 hours to obtain a homogenous solution. After 3 hours of mixing, the PCBM solution was ready to implement on perovskite material. PCBM was spin coated on perovskite at 1000 rpm for 30 s. So, the top layer of the solar cell was completed.

3.2.1.4. Back Electrode. The last step of perovskite solar cell manufacture is the back electrode attachment. As it can be seen in the Figure 3.1, this design has both Al and Cu tape cathode. The solar cell was finished by the lamination process of conductive tapes. The Al and Cu tapes were attached on PCBM. Then, the roll to roll process was applied to ensure that the tapes were properly attached and there was no air in between tape and PCBM layer. The roll to roll process is shown in Figure 3.4. The fabricated solar cell is displayed in Figure 3.5 below. (Shao *et al.*, 2015)

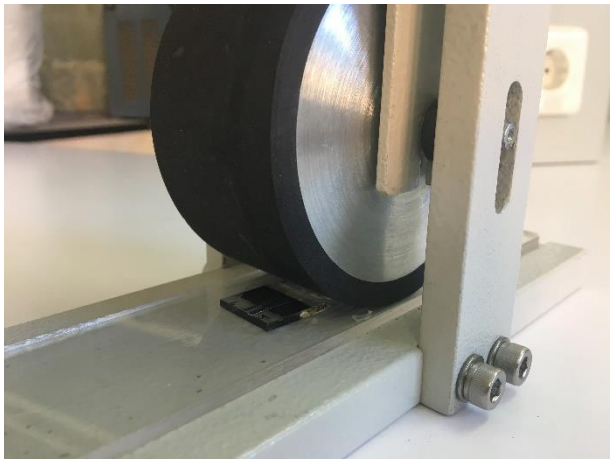

Figure 3.4. Roll-to-Roll Process.

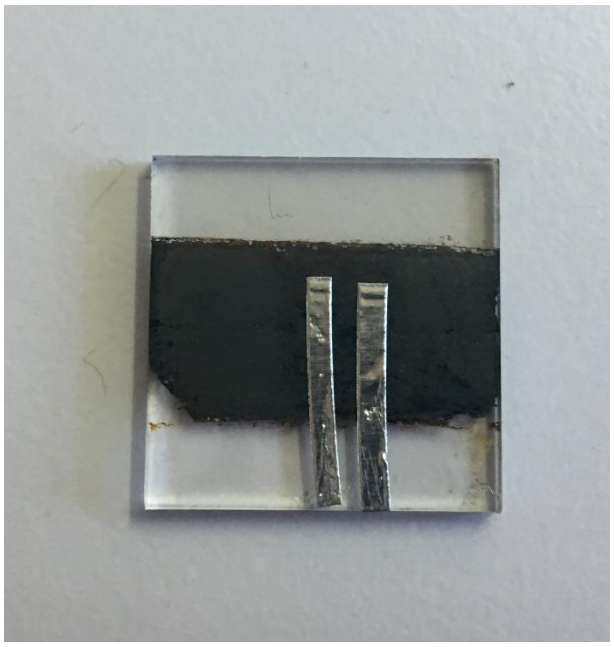

Figure 3.5. TiO_2 as ETL and PCBM as HTL solar cell with Al tape.

3.2.2. Solar Cells with TiO_2 as ETL and ZnO as HTL

The solar cell structure was designed that TiO_2 is electron transport layer and ZnO is hole transport layer. TiO_2 was coated on FTO glass substrate. After perovskite deposition on TiO_2, ZnO was spin coated on perovskite layer. Then, Al tape as a back electrode was attached to the surface of the solar cell. This cell differentiated from the former cell with the perovskite deposition method and conductive top layer of the cell. Figure 3.6 shows the cell structure in detail.

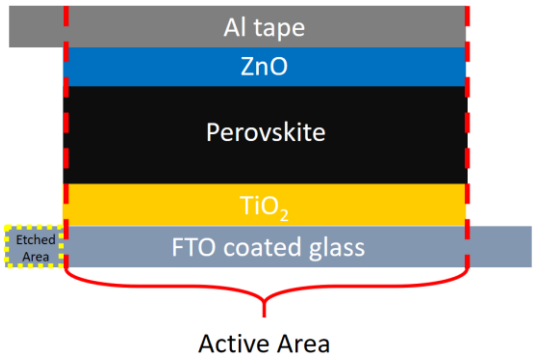

Figure 3.6. TiO_2 as ETL and ZnO as HTL solar cell structure with Al tape back electrode.

3.2.2.1. Cleaning of FTO and TiO_2 Coated Glass Substrates. The solar cell which has TiO_2 electron transport layer and ZnO hole transport layer was fabricated by applying cleaning, perovskite deposition, ZnO deposition, and finally Al cathode addition steps. Because TiO_2 was already coated on the FTO glass, and the substrate was etched, only cleaning of the glass was required. Similar to the former solar cell fabrication, the glass was washed with distillate water and ethanol. It was dried under nitrogen to remove any dust remains on the surface. Then, the FTO and TiO_2 coated glass was ready to perovskite deposition step.

3.2.2.2. Perovskite Synthesis via 2-step Deposition Method. Perovskite layer was produced by 1-step deposition method mixing PbI_2 and CH_3NH_3I in DMF, and using the resulting solution to cover the substrate by spin coating. In contrast, 2-step deposition method involves two solutions which are coated on the glass separately.

First, 460 mg PbI_2 was dissolved in 1 ml DMF at 100℃. The mixture was stirred at that temperature for minimum 10 minutes using magnetic stirrer, until all PbI_2 was completely solved by DMF. Then, the solution of PbI_2 was spun on TiO_2 layer at a speed of 3000 rpm for 10 s. After coating PbI_2, the substrate was placed on hot plate and annealed at 100℃ for 10 minutes. After annealing, PbI_2 coating appeared as homogeneous yellow layer. (You *et al.*, 2015)

The second step of the perovskite deposition process is the application of CH_3NH_3I solution on PbI_2 layer. Methylammonium iodide was dissolved in 2-propanol with a concentration of 50 mg/ml. The solution was stirred for minimum 10 minutes. Then, CH_3NH_3I solution was spun on PbI_2 layer with a speed of 4000 rpm for 20 s. After spin

coating, the coated glass was placed on hot plate and annealed at 100℃ for 2 hours. At the beginning of annealing process, the color of perovskite material became brown or black indicating proper perovskite crystal formation. (You et al., 2015)

3.2.2.3. ZnO Deposition. ZnO nanoparticles dispersed in butyl acetate with 40% (in weight) concentration was deposited on perovskite to create a conductive layer. ZnO was spin coated at a speed of 2500 rpm for 30 s. Then, annealing was applied at 150℃ for 10 minutes. During this process, perovskite changed its color from brown or black to yellow due to effect of butyl acetate on perovskite structure.

3.2.2.4. Back Electrode. Al tape was used as back electrode which is the last step of the solar cell. The solar cell was completed by the lamination process of Al conductive tape. In order to provide better adhesion, roll to roll process was performed on the tape.

3.2.3. Solar Cells with NiO as HTL and ZnO as ETL

The perovskite solar cell structure consists of NiO as hole transport material and ZnO as electron transport layer. ITO coated glass was used as anode of the cell. On the ITO layer, NiO was coated to be used as hole transport layer. Then, perovskite was synthesized by using both 1-step and 2-step deposition methods. In order to provide electron movement through the solar cell, ZnO was spin coated on perovskite material. The final step of solar cell fabrication is the cathode formation on electron transport layer. Both Al tape and Cu tape was utilized as back electrode. In addition, Au was sputtered on ZnO layer forming another cathode type. The design of this solar cell is shown in Figure 3.7.

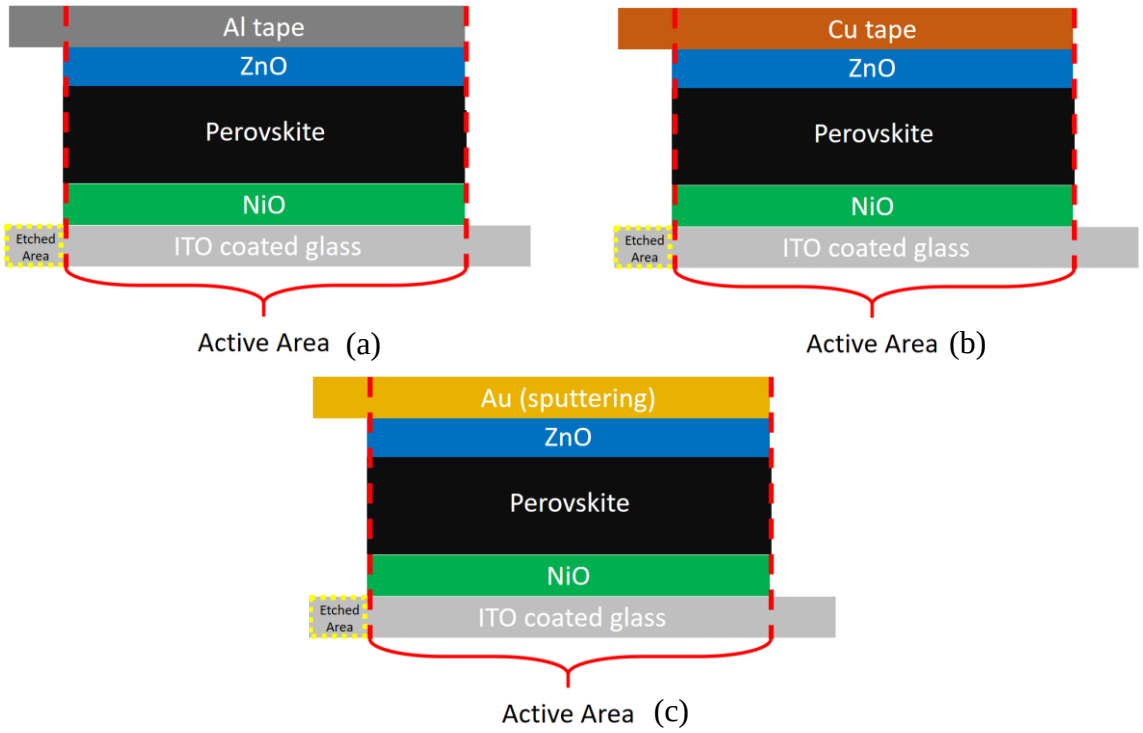

Figure 3.7. NiO as HTL and ZnO as ETL solar cell structure with (a) Al tape back electrode, (b) Cu tape back electrode, (c) Au (sputtering) electrode.

3.2.3.1. Etching and Cleaning of ITO Coated Glass Substrates. ITO coated glasses should have uncoated areas to avoid short circuit formation in the solar cells. So, some part of ITO on the glass substrates were etched from the surface. Etching process was applied by using Zn powder and HCl solution with 37% concentration. The ITO coated area that was not etched, was covered with paper tape. On the other hand, undesired ITO coated area was covered with Zn powder. The ITO glass substrate loaded with Zn powder was heated to 70℃ placing on the hot plate.

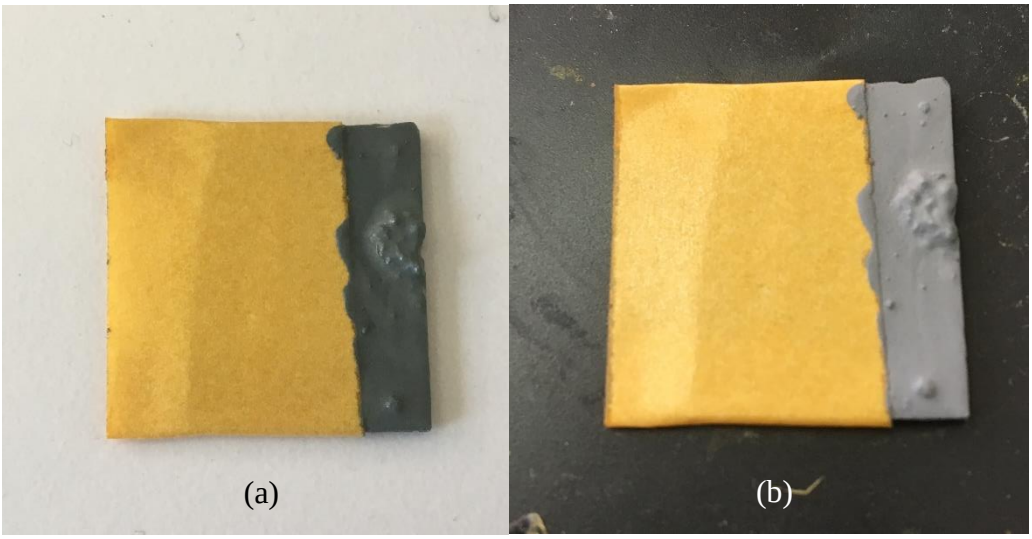

Figure 3.8. Zn loaded ITO glass (a) before heating, (b) after heating.

The heated glass was dipped into HCl solution, which resulted in the reaction between Zn and HCl solution. During the reaction, ITO was etched from the surface of the glass. Then, the tape which was used to protect the desired ITO coated area was removed. Etching process is displayed in detail in Figure 3.9.

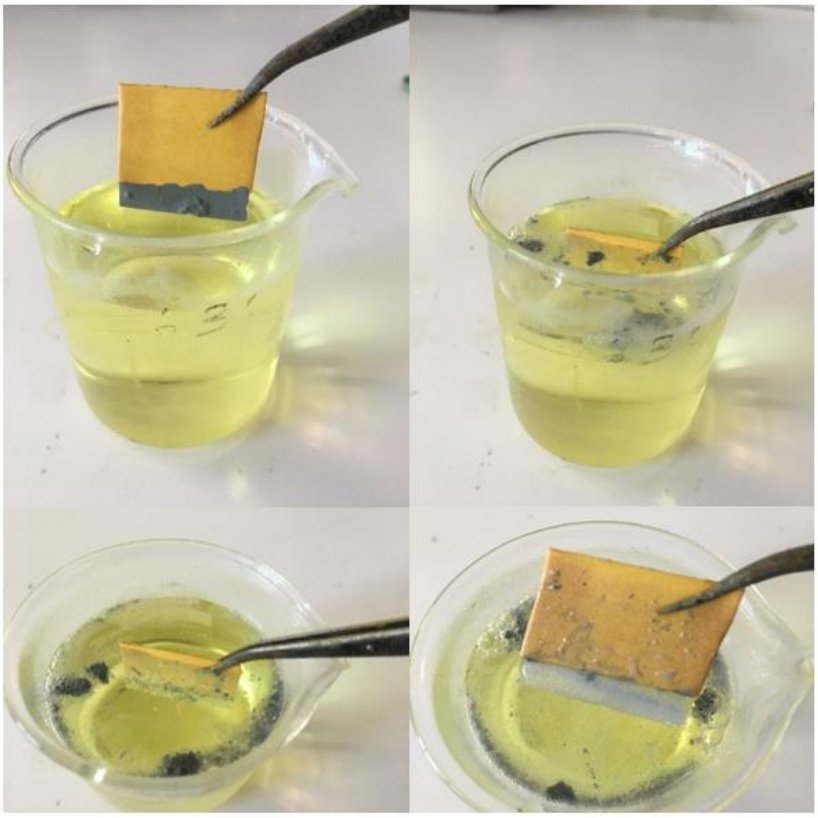

Figure 3.9. Dipping into HCl solution and etching process.

The glass was cleaned with distillate water and ethanol under ultrasound for 5 minutes, respectively.

Figure 3.10. Cleaning etched substrates.

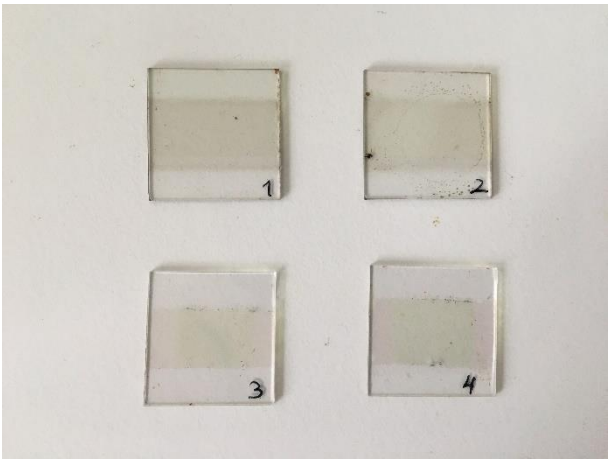

Figure 3.11. Etched ITO coated glasses.

3.2.3.2. Synthesis and Deposition of NiO. NiO is a conductive material that was used for hole transporting in the solar cell. During experiments, NiO was produced by two different methods to implement on ITO surface. In order to synthesize NiO, Nickel Acetate Tetrahydrate was used in both procedures.

First, 0.37 g Nickel Acetate Tetrahydrate was dissolved in 10 ml 2-Methoxyethanol. The mixture was stirred for 1 hour at 60℃ using magnetic stirrer. After obtaining

homogeneous green solution, 0.01 ml HCl was added to the solution. Then, the solution was kept under standard conditions for 24 hours for aging of the solution. The NiO solution was ready to use after 24 hours of waiting. (Purushothaman *et al.*, 2011)

The second method is differentiated from the previous one with the use of different solvent for NiO manufacture. 0.25 g Nickel Acetate Tetrahydrate and 0.06 ml Monoethanolamine were dissolved in 10 ml ethanol. The mixture is stirred at 70℃ for 4 h. After 4 hours of mixing, homogenous and deep green solution appeared. (Docampo *et al.*, 2013; Manders *et al.*, 2013)

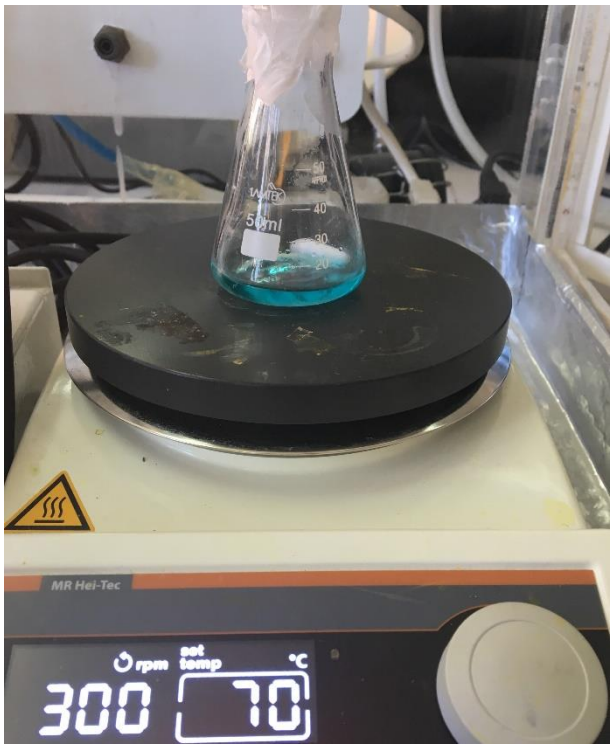

Figure 3.12. NiO solution preparation.

After NiO solution was prepared, ITO glass substrates were coated with NiO. In order to prevent the NiO formation on etched area, paper tape was attached to etched region of the glass. Then, NiO was spin coated at a speed of 2500 rpm for 15 s, and coated glass substrates were placed on a hot plate. The NiO coated glasses were heated for 2 minutes at 350℃. Then, the NiO coated glass was again coated with NiO. The same coating procedure was repeated for 4, 5, 6, 8 and/or 10 times targeting different thickness of NiO layers (Purushothaman *et al.*, 2011). After repeating the procedure to get desired thickness, the

glasses were kept at 350℃ for 1 hour to stabilize the NiO layer. By this way, both desired thickness was achieved and NiO was uniformly coated on the surface of the ITO layer. Moreover, the most common thickness of NiO layer of solar cell samples were obtained by repeating the coating 4 times on ITO glass.

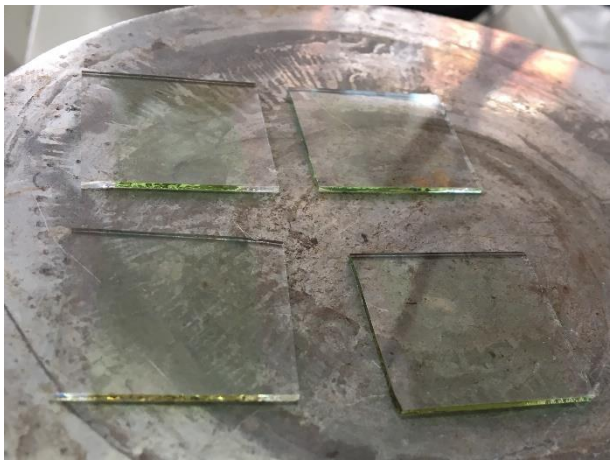

Figure 3.13. NiO coated glasses on a hot plate.

3.2.3.3. Perovskite Synthesis with 1-step and 2-step Deposition Methods. The fabrication of NiO based p-i-n type solar cells were followed by generation of perovskite layer on NiO hole transport material. The perovskite was formed by using both 1-step and 2-step deposition methods that was mentioned in previous sections. The perovskite precursor preparation is the same as it was explained in sections 3.2.1.2 and 3.2.2.2, however it was applied on NiO instead of TiO_2 layer.

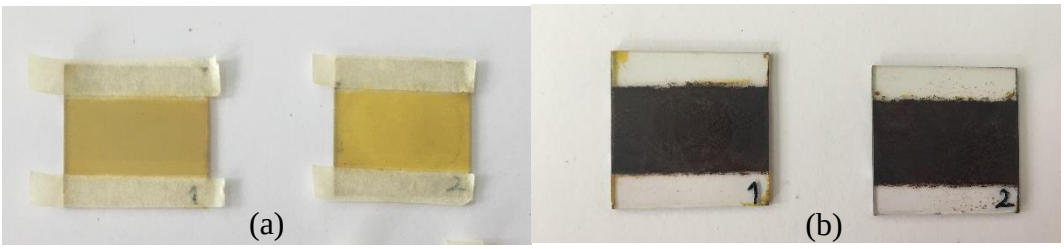

Figure 3.14. 2-step deposition of perovskite (a) shows PbI_2 coating (b) MAI coating.

1-step deposition method was used in solar cells, which had 6 and 10 layers of NiO covering. On the other hand, 2-step deposition of perovskite was applied on all options of NiO thicknesses to observe the effect of hole transport layer thickness on the performance of the cell.

3.2.3.4. ZnO Deposition. ZnO nanoparticles dispersed in butyl acetate were deposited on perovskite to form electron transport layer. ZnO was spin coated at a speed of 2500 rpm for 30 s. Then, ZnO coated glass substrate was annealed at 150℃ for 10 minutes.

3.2.3.5. Back Electrode. Al tape, Cu tape and Au by sputtering were applied to form cathode of the cell. Al tape was used in perovskite solar cells with 4, 5, 6, 8, and 10 layers of NiO coating and 2-step deposited perovskite layer. Also, the solar cells which had perovskite deposited by 1-step method with 6 and 10 layers of NiO in the structure used Al tape as back electrode.

In addition, both Cu tape and sputtering of Au was implemented on solar cells having perovskite layer produced by 2-step deposition method and 4 layers of NiO covering. Both perovskite and NiO options were the most commonly used structures.

Al and Cu tapes were attached to the surface of ZnO layer. Then, roll-to-roll mechanism was utilized to have smooth cathodes. On the other hand, sputtering of Au was performed by Sputter Coater in Boğaziçi University Advanced Technologies Research Center. While coating the solar cell sample with Au, Sputter Coater had 1.6 kV voltage and 27 mA plasma current.

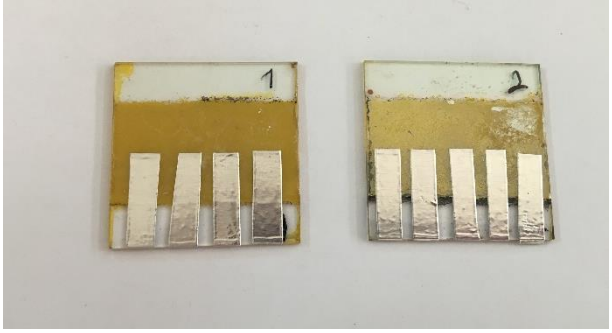

Figure 3.15. ZnO coated and Al tape attached solar cells.

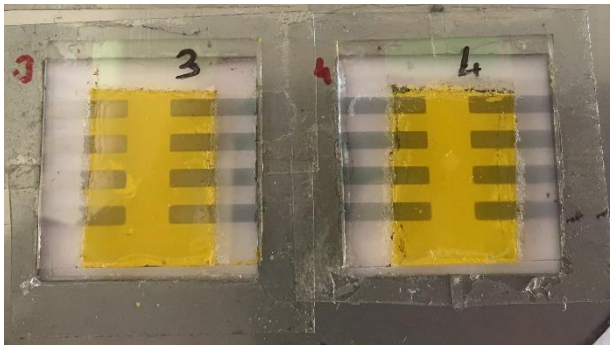

Figure 3.16. ZnO coated and Au sputtered solar cells.

3.2.4. Solar Cells with NiO as HTL and Ionic Liquid as ETL

These perovskite solar cells have NiO as hole transport material and ionic liquid as electron transport material. The ionic liquid used was 1-Ethyl-3-methylimidazolium bis (trifluoromethylsulfonyl)imide. The solar cells were developed similar to the previous cell structure. First, ITO coated glasses were covered with NiO layers. Then, perovskite was deposited by 2-step fabrication method. On the perovskite layer, a highly conductive ionic liquid was performed as electron transport material. The perovskite solar cell design was completed with Al and Cu tape lamination process. The design of the solar cell is displayed in Figure 3.17.

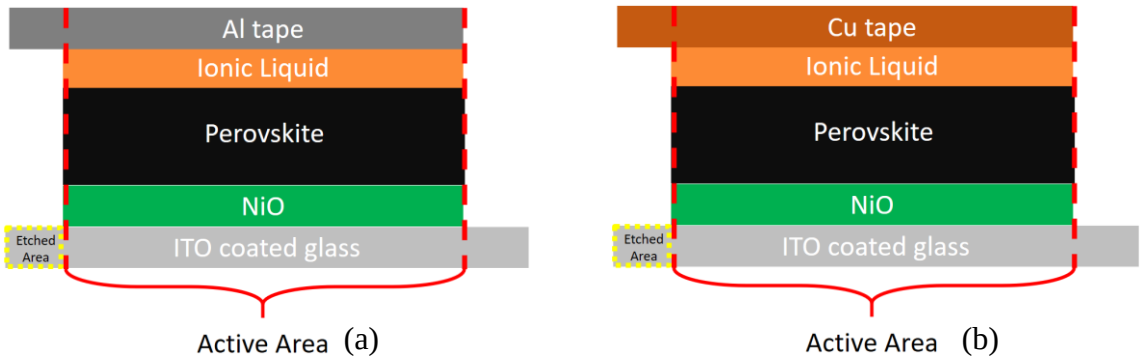

Figure 3.17. NiO as HTL and Ionic Liquid as ETL structure (a) Al tape back electrode (b) Cu tape back electrode.

3.2.4.1. Etching and Cleaning of ITO Coated Glass Substrates. ITO coated glasses were etched using Zn powder and HCl solution by the help of Zn and HCl reaction which was explained in section 3.2.3.1. As mentioned before, in order to get rid of the Zn, HCl and tape residuals on the surface of the glasses, ITO coated substrates were washed with distillate

water and ethanol under ultrasound for 5 minutes, respectively. Then, the glasses were dried under nitrogen to remove any dust from the surface.

3.2.4.2. Synthesis and Deposition of NiO. NiO was used as hole transport material. First NiO solution was produced with the same procedure explained in previous sections. After NiO solution was prepared, ITO glass substrates were coated with NiO by spin coating at 2500 rpm for 15 s. Then, coated glasses were put on a hot plate for 2 minutes at 350℃. Afterwards, the coating and annealing of NiO was repeated to obtain 4 layers of NiO on ITO glasses. When the get desired thickness was achieved, the NiO coated glasses were annealed at 350℃ for 1 hour to stabilize the NiO layer.

3.2.4.3. Perovskite Synthesis via 2-step Deposition Method. The perovskite was fabricated by 2-step deposition method. First, 460 mg/ml PbI_2 solution was spun on NiO layer at 2500 rpm for 15 s and annealed at 100℃ for 10 minutes. Afterwards, 50 mg/ml MAI solution in 2-propanol was spin coated on PbI_2 layer at 2500 rpm for 20 s in ambient air. Annealing of perovskite was carried out at 100℃ for 2 hours on a hot plate.

3.2.4.4. Ionic Liquid Deposition. The ionic liquid used was 1-Ethyl-3-methylimidazolium bis (trifluoromethylsulfonyl)imide due to its high ionic conductivity property. The ionic liquid was spin coated on perovskite layer with a speed of 2500 rpm for 20 s. Then, it was annealed at 150℃ for 10 minutes. However, perovskite was damaged due to ionic liquid effect on perovskite structure while heating. So, annealing process was not performed after spin coating.

3.2.4.5. Back Electrode. Al and Cu tapes were attached to the solar cell as the last step of the solar cell fabrication. They were used as back electrode of the cell structure. The lamination process of Al and Cu tapes were followed by roll-to-roll method application on the electrodes to complete the solar cell.

3.2.5. Solar Cells with NiO as HTL and without ETL

The perovskite solar cell structure normally has a hole transport layer and an electron transport layer. Perovskite layer is located in between HTL and ETL. However, since

perovskite provides smooth electron movement in its structure, perovskite solar cells without electron layers were also fabricated. Figure 3.18 shows the details of ETL free perovskite solar cell structure. The structure of ETL free solar cell is similar to ZnO-ETL structure. Therefore, the same procedure steps were followed while producing the solar cells.

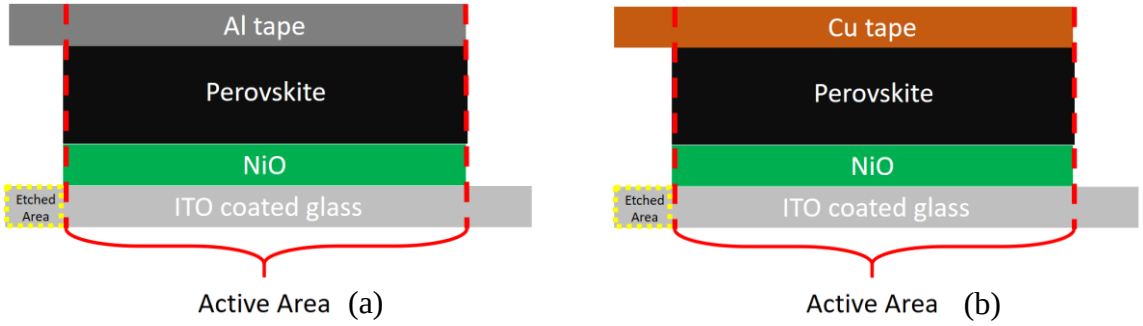

Figure 3.18. NiO as HTL and without ETL structure (a) Al tape back electrode (b) Cu tape back electrode.

3.2.5.1. Cleaning and Etching of ITO Coated Glass Substrates. The same steps for etching and cleaning of ITO substrates were followed. The samples were etched with HCl and Zn reaction and then the ITO coated glasses were washed with distillate water and ethanol under ultrasound for 5 minutes.

3.2.5.2. Synthesis and Deposition of NiO. NiO solution was prepared with the same procedure explained before. Then, NiO solution was spun on ITO substrates by spin coating at 2500 rpm for 15 s and annealed at 350℃ for 2 minutes. Then, the same steps were repeated for 4, 5, 8 and/or 10 times aiming various thicknesses of NiO layers. Finally, substrates were annealed at 350℃ for 1 hour. The perovskite was synthesized both 1-step and 2-step deposition method on NiO layer. The cell which had perovskite with 2-step deposition method used 4, 5, 8 and 10 layers of NiO in its structure. Whereas, the cells with 1-step deposited perovskite was fabricated by using 4 or 5 layers of NiO. The thickness influenced the performance of the perovskite solar cells.

3.2.5.3. Perovskite Synthesis with 1-step and 2-step Deposition Methods. The perovskite production is the key element of the solar cell generation. Perovskite was produced by both 1-step and 2-step deposition methods. 1-step deposited perovskite solar cells had 4 and 5

layers of NiO while the perovskite solar cells fabricated by using 2-step deposition method used 4, 5, 8, and 10 layers of NiO as hole transport layer thicknesses.

3.2.5.4. Back Electrode. The final step of solar cell was the addition of back electrode. This design used Al and Cu tape electrodes which were directly attached to the surface of the perovskite layer. There was no electron transport layer between perovskite layer and the cathode. Lastly, the roll-to-roll process was conducted to get smooth adhesion.

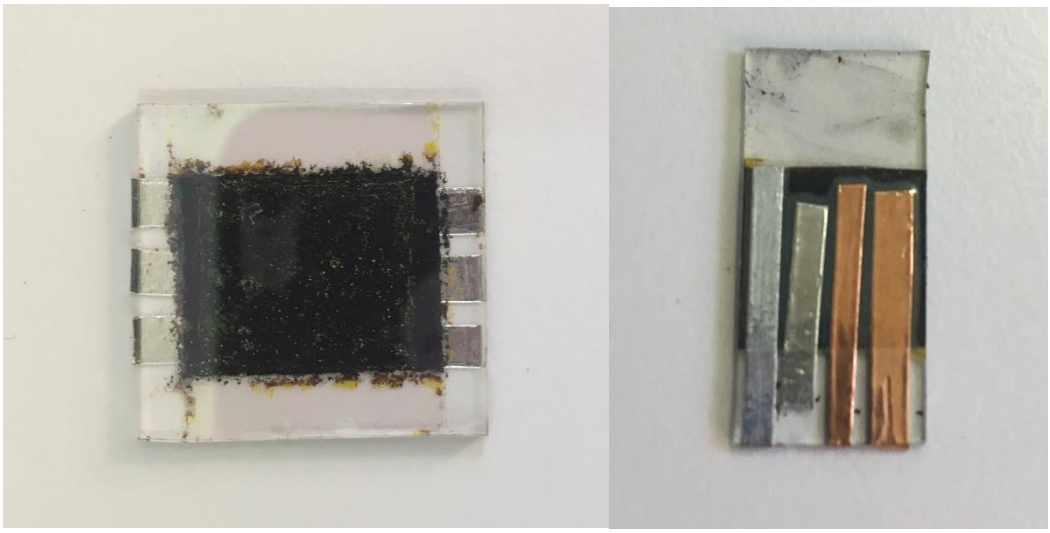

Figure 3.19. ETL free solar cells with Al and Cu tape attached.

3.3. Characterizations of Perovskite Solar Cell

3.3.1. Electrical Characterization of Perovskite Solar Cells

The electrical characteristics of solar cells were performed by Keithley Instruments Series 2401 Source Meter controlling with a computer program LabTracer 2.9 under AM 1.5G illumination at 100 mW/cm^2 irradiance of LS 150 Xenon Lamp Source ABET solar simulator. The I-V measurements were conducted by scanning from 0 V to 1 V with 200 ms delay time and from -1 V to 1 V with 200 ms delay time under illumination. The I-V curve and power curve were obtained for each solar cell.

The photovoltaic characteristics of a cell are determined by performing measurements under illumination. The parameters that should be specified are open circuit voltage (V_{OC}),

short-circuit current (I_{SC}), and fill factor (FF) to obtain the power conversion efficiency (η) of a cell. Open circuit voltage is the highest voltage value that a cell can provide. V_{OC} is observed where the current is zero. Moreover, short circuit current is the highest current of a solar cell obtained at the point where the I-V curve has zero voltage. Also, short circuit current density (J_{SC}) is another element that indicates the current production of the cell. It represents the current per area of the cell with zero voltage conditions. In addition, I_{MP} is the current at maximum power point and V_{MP} is the voltage observed at maximum power point. These variables enable to determine the performance of the solar cell.

Fill factor is a parameter that is connected with open circuit voltage, short circuit current, and maximum power elements. FF demonstrates the quality of the solar cell. In other words, FF is the measurement of squareness of I-V curve. The high FF means that curve is squarer and solar cell has high quality standards. The calculation of FF is shown in the equation.

$$FF = \frac{P_{max}}{V_{OC} I_{SC}} = \frac{V_{MP}.I_{MP}}{V_{OC}.I_{SC}} \tag{3.1}$$

Figure 3.20 displays an I-V curve example containing all voltage and current parameters. The open circuit voltage, maximum power voltage, short circuit current, and maximum power current are located in the 4th quadrant of the I-V curve. The green area represents the maximum power that can be produced by the solar cell.

The characterization of a solar cell is followed by determination of the power conversion efficiency. The efficiency of the cell is the most important indicator of the performance of the device. A solar cell may have high V_{OC} or I_{SC} which indicates the solar cell mechanism is working. However, overall performance of the cell can be decided according to PCE of the device. Calculation of PCE is given in the following equation which includes FF, V_{OC}, I_{SC} and P_{light} parameters. P_{light} indicates the power of the light during illumination which is 100 mW/cm^2.

$$PCE = \eta = \frac{FF.V_{OC}.I_{SC}}{P_{light}} \tag{3.2}$$

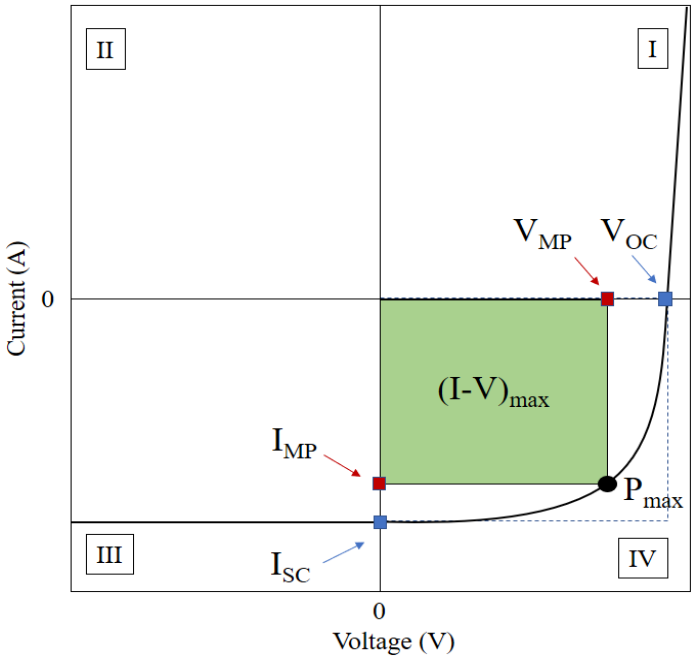

Figure 3.20. I-V curve of a solar cell.

3.3.2. Structural Characterization of Perovskite Solar Cells

SEM (Scanning Electron Microscope) analysis of methylammonium iodide perovskite solar cells fabricated by one-step and two-step perovskite deposition methods was performed by using Philips XL30 ESEM-FEG/EDAX system in Boğaziçi University Advanced Technologies Research Center.

4. RESULTS AND DISCUSSION

4.1. TiO_2 as ETL and PCBM as HTL Structure

TiO_2 is the most commonly used electron transport material in perovskite solar cells. Therefore, solar cell with TiO_2 as ETL was one of the solar cell designs used in this work. FTO substrates coated with TiO_2 ETL were covered with perovskite by applying one-step deposition method. $MAPbI_3$ was prepared having 3:1 molar ratio of MAI:PbI_2 precursor solution in DMF. The precursor solution was spin coated and then annealed at 90℃ for 2 hours to form perovskite layer. Since there was excess amount of MAI, surface coverage of perovskite was sufficient for reducing pin hole formation. Low PbI_2 amount in perovskite precursor suppresses the microfiber generation due to unreacted PbI_2 crystallization. Therefore, the precursor ratio leads smooth coverage whereas the performance of solar cell was poor. PCBM was applied on the perovskite surface and solar cell was finished with Al tape attachment. PCBM is mostly employed as electron transport material in solar cells. However, in this configuration it acted as hole transport material causing poor performance and low open circuit voltage.

Cu tape containing solar cell was fabricated following the same procedure that Al taped solar cell. Although the only parameter changed was the cathode of the cell, electrical properties of Al and Cu tape involving cells were varied from each other. Cu taped solar cell has higher efficiency than Al tape having cells. This may stem from the perovskite crystal formation under atmospheric environment due to moisture effect even the procedure was the same. Moreover, the efficiency of devices is inversely proportional to the active area. Hence, high performance of Cu tape containing cell may come from the small active area. Also, Cu is a better conductive material than Al.

The efficiencies of TiO_2/$MAPbI_3$/PCBM/Al and TiO_2/$MAPbI_3$/PCBM/Cu structured solar cells are very low when it is compared to PCE values from the literature. A solar cell with TiO_2 ETL, one-step deposited perovskite layer and a HTL could obtain 12.16 % (Huang *et al.*, 2016) and 6.83 % (Yang *et al.*, 2016) efficiency. The efficiency of the solar cells that were fabricated using PCBM was expected to be close to the results of studies of Huang *et*

al. and Yang e*t al.*. However, TiO_2/$MAPbI_3$/PCBM/Al and TiO_2/$MAPbI_3$/PCBM/Cu configurated solar cells could only reach 2.61×10^{-5}% and 1.21×10^{-4}% power conversion efficiencies, respectively. The solar cell examples from literature have similar fabrication methods with the solar cells of this study. The only difference is the choice of top layer which was PCBM in this study while Huang *et al.* and Yang e*t al.* used spiro-OMeTAD as hole transporting material. Also, the back electrode that was used in this study was Al and Cu conductive tapes. In contrast, Huang *et al.* and Yang e*t al.* deposited back electrode via thermal evaporation of Ag. The experimental results that were obtained from the TiO_2/$MAPbI_3$/PCBM/Al and TiO_2/$MAPbI_3$/PCBM/Cu structures are 0.11 and 0.14 V of V_{OC}, 1.45×10^{-3} and 3.92×10^{-3} mA/cm^2 of J_{SC}, and 16.2 and 21.2 % of FF, respectively. However, Huang *et al.* obtained V_{OC} as 0.97V, J_{SC} as 19.03 mA/cm^2, and FF as 66% while the electrical characterization results which were V_{OC} as 0.85V, J_{SC} as 11.51 mA/cm^2, and FF as 70% were achieved by Yang *et al.* (Huang *et al.*, 2016; Yang *et al.*, 2016). According to the electrical characteristics of solar cells in literature, the experimental results are very low. There are several causes that lead poor device performance. First, in this study $MAPbI_3$ was synthesized in air being exposed to both moisture and oxygen. This was the main problem that caused low efficiency of perovskite solar cells. Secondly, the top layer of perovskite solar cells was PCBM in this study, which was an ETM but used as HTM. Due to poor hole transport property of PCBM, recombination of electron and hole got faster. As a result, voltage and the current density that was obtained from cells were relatively low. Finally, the back contact of the solar cells in literature was made by thermal evaporation method with a thin layer of Ag, whereas Al and Cu tapes were applied as back electrode of perovskite solar cells in this study. The thick metal tapes caused electrical resistance decreasing the current density of the solar cells.

The J-V and P-V curve of TiO_2/$MAPbI_3$/PCBM/Al structure is displayed in Figure 4.1 and Figure 4.2. In addition, the J-V and P-V curve of TiO_2/$MAPbI_3$/PCBM/Cu structure is displayed in Figure 4.3 and Figure 4.4, respectively. Also, electrical properties such as short circuit current density, open circuit voltage, FF, and PCE of the cell configurations that were determined from the graphs are listed in Table 4.1.

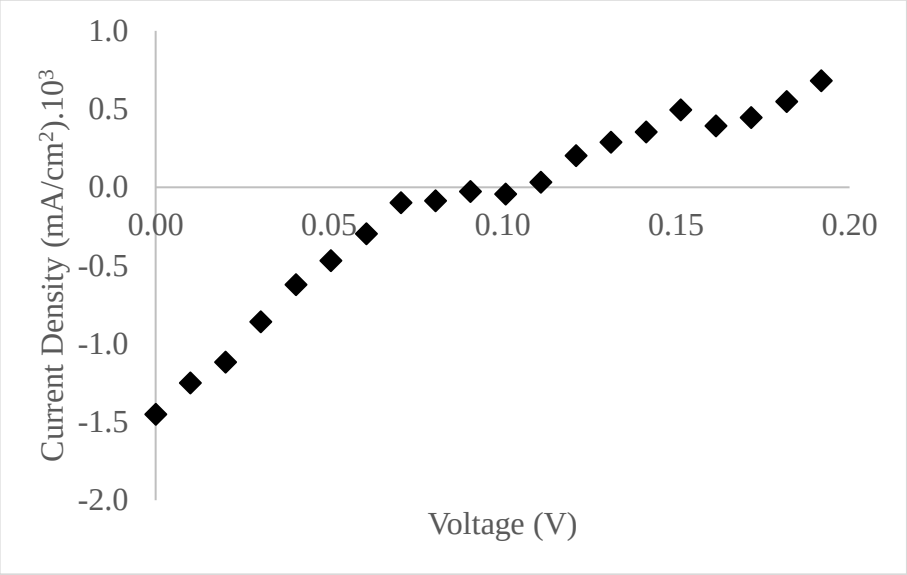

Figure 4.1. J-V curve of $TiO_2/CH_3NH_3PbI_3$/PCBM/Al structure.

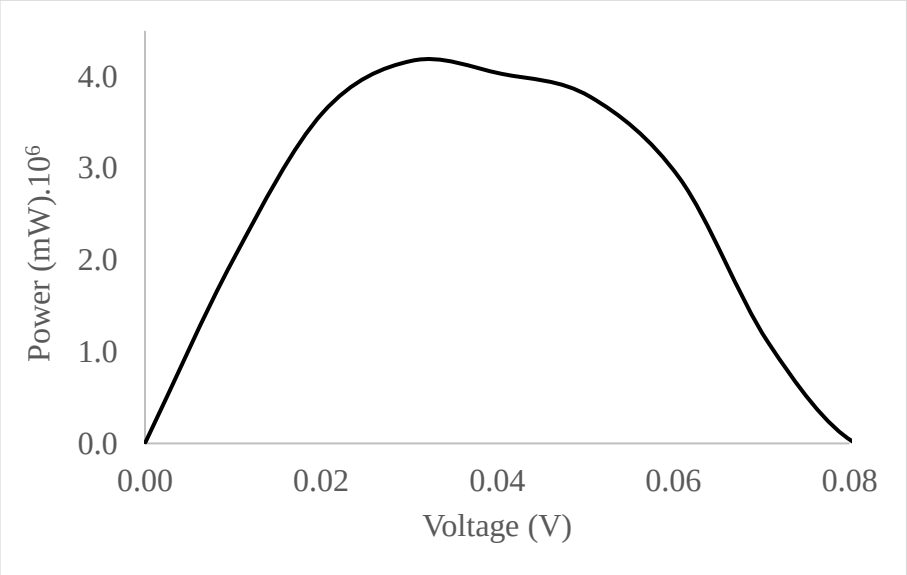

Figure 4.2. P-V curve of $TiO_2/CH_3NH_3PbI_3$/PCBM/Al structure.

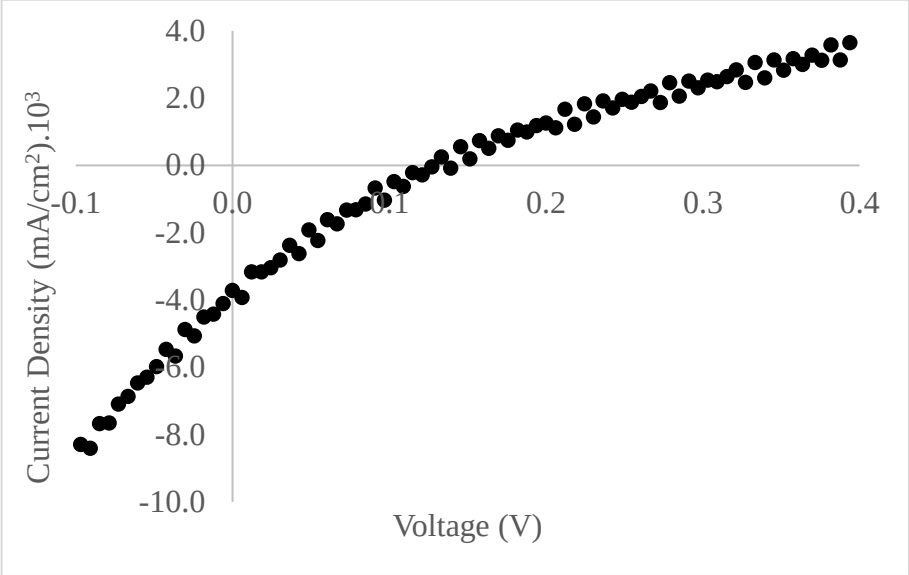

Figure 4.3. J-V curve of $TiO_2/CH_3NH_3PbI_3$/PCBM/Cu structure.

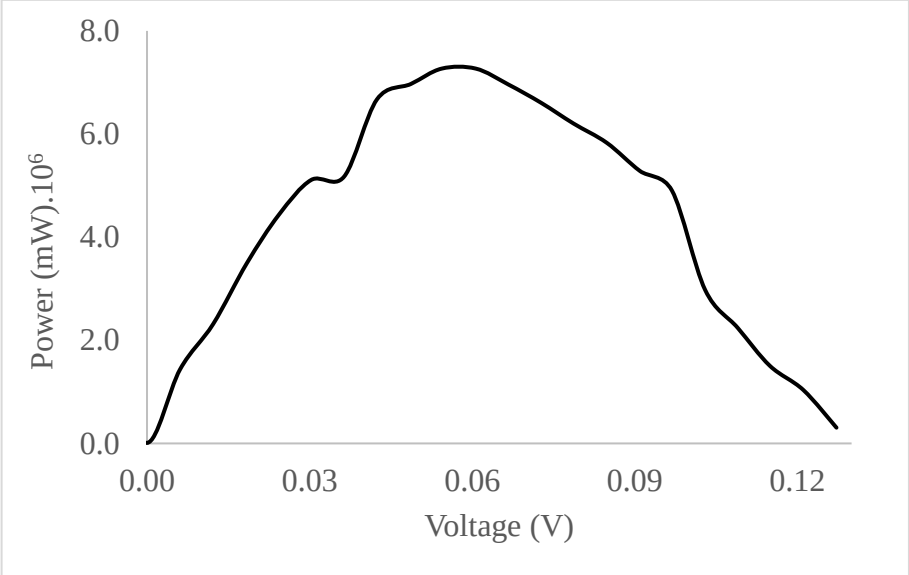

Figure 4.4. P-V curve of $TiO_2/CH_3NH_3PbI_3$/PCBM/Cu structure.

Table 4.1. Performances of PCBM as HTL devices.

Device Configuration	PCE (%)	FF (%)	J_{SC} (mA/cm^2)	V_{OC} (V)	Active Area (cm^2)
FTO / TiO_2 / Perovskite / PCBM / Al	2.61×10^{-5}	16.2	1.45×10^{-3}	0.11	0.16
FTO / TiO_2 / Perovskite / PCBM / Cu	1.21×10^{-4}	21.2	3.92×10^{-3}	0.14	0.06

4.2. TiO_2 as ETL and ZnO as HTL Structure

Perovskite solar cells with TiO_2 electron transport layer was fabricated by spin coating of all necessary layers. $MAPbI_3$ perovskite was synthesized by one-step deposition method applying the 3:1 ($MAI:PbI_3$) molar ratio precursor solution on TiO_2 coated FTO substrate. This followed by annealing at 90℃ for 2 hours. Then, ZnO was coated on perovskite layer. Al tape was applied as cathode of the solar cell.

The solar cell generation is similar with the device in previous section. However, the conductive layer PCBM was replaced with ZnO. The device performance was already poor because of one-step deposition of perovskite. In addition, ZnO may cause degradation of perovskite by interaction between perovskite material and ZnO. Also, ZnO was dispersed into butyl acetate which partially dissolves the perovskite. As a result, $TiO_2/MAPbI_3/ZnO/Al$ configuration could not produce any electrical power.

4.3. NiO as HTL and ZnO as ETL Structure

Perovskite solar cells with inverted planar configuration were fabricated using NiO as HTM and ZnO as ETM. These inorganic charge transport materials were used since they have high carrier mobility and improved stability in ambient air.

The construction of the cells was initiated with etching and cleaning of the ITO substrates in order to prevent short circuit in the solar cell. Then, the prepared NiO solution was coated on ITO substrate by spin coating. However, NiO could not form a continuous coverage on ITO substrate. Thus, NiO solution was spun for several times obtaining 4, 5, 6, 8, and 10 layers of NiO. By this way, the thickness of NiO film was also controlled.

After NiO coverage, perovskite was deposited by either single step or sequential deposition methods. Although one-step deposition method was valid for TiO_2 based solar cells, NiO based perovskite solar cells did not work due to deficiency of perovskite structure. Because of rough surface of NiO material, perovskite could not form smooth surface. As it can be seen in Figure 4.5, the single step deposition caused an island like perovskite formation on NiO surface. When the island like structure is investigated, perovskite crystals

can be observed with large grain sizes. Larger crystals provide decrease in charge recombination improving the efficiency of perovskite layer. Even it was hard to obtain continuous coverage, NiO provided improved crystallinity of perovskite with larger grain size. It can be said that one-step deposition method can form perovskite crystals with high quality, but the perovskite could not cover the whole surface of the conductive layer due to moisture and oxygen influence on the crystallization. Because of weak surface coverage, single step perovskite synthesis causes poor performance of the cell.

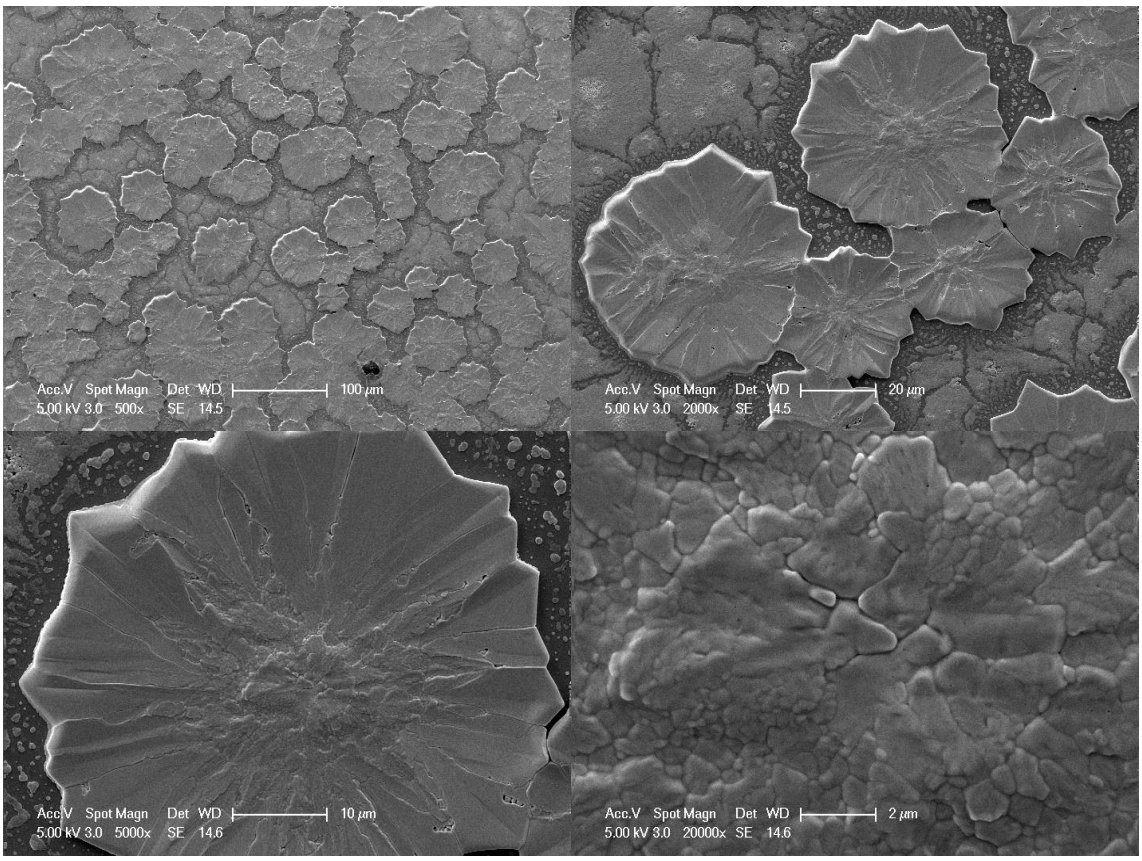

Figure 4.5. SEM image of perovskite growth on NiO surface by 1-step deposition method.

In order to overcome weak surface coverage problem, sequential deposition of perovskite film was employed on NiO layer. According to the Figure 4.6, it can be said that the surface coverage of perovskite film is successful in two step deposition method. There is no observable pin hole or island formation on the perovskite. The perovskite material covered the whole conductive layer. The closer pictures show that the perovskite uniformly distributed on the surface creating smaller crystals. Since perovskite layer synthesized by sequential deposition had high quality perovskite film, the performance increases.

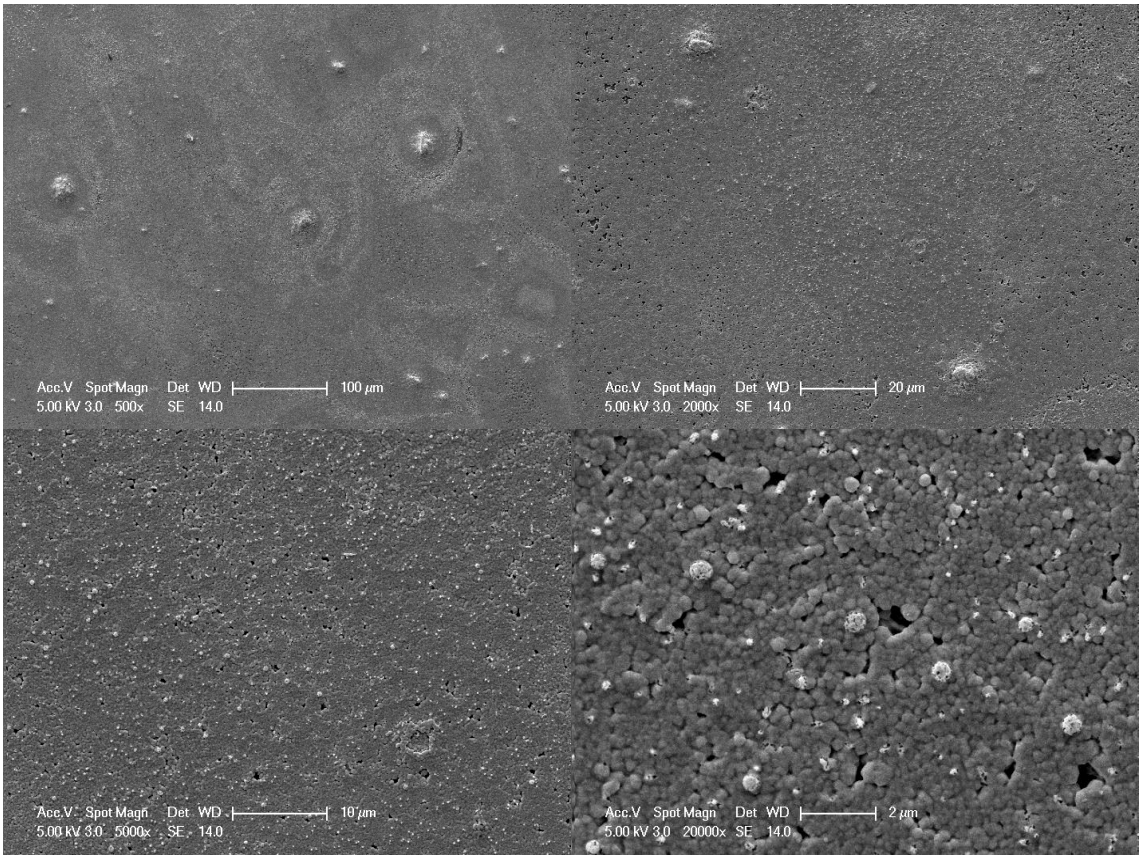

Figure 4.6. SEM image of perovskite growth on NiO surface by 2-step deposition method.

ZnO was applied as electron transport material on the perovskite solar cell. Perovskite deposited substrate was coated with ZnO by spin coating. ZnO is an efficient electron transport material with strong electron blocking properties, which provides decline in charge recombination and increased current density. Also, the top layer of perovskite, which was ZnO, could preserve the perovskite structure from moisture and oxygen exposure by coating the surface with high quality film of ZnO. On the other hand, ZnO may induce defects in perovskite structure reducing the performance of the cell because of interactions between nanoparticles of ZnO and perovskite. The annealing of ZnO layer was resulted in color change of perovskite layer from black to yellow indicating that perovskite structure was partially damaged. This caused diminished efficiency of perovskite solar cell.

The last step of perovskite solar cell production was back electrode addition. In the experiments, Al and Cu tapes were used as cathode of the cell structure. Also, Au was sputtered on ZnO to be used as back electrode of the solar cell.

The structure of perovskite solar cell can be seen in Figure 4.7. According to the images, layer thicknesses can be measured. Layer thicknesses of NiO (4 layers), perovskite and ZnO is approximately 625 nm, 800 nm and 250 nm, respectively. The back electrode of solar cell in figures was not included. The thickness of NiO, perovskite and ZnO layers are greater when it is compared to literature. You *et al.* fabricated the same solar cell structure with 80 nm, 320 nm, and 70 nm thicknesses respectively achieving 16.1% PCE (You *et al.*, 2015). In this study, the efficiency is far below the literature value, which may originate from large film thicknesses of layers reducing the performance of HTL, perovskite and ETL. Large NiO layer causes increased electrical resistance reducing fill factor. In contrast, if NiO layer is very thin, current leakage may occur causing drop in open circuit voltage and FF values due to insufficient film of NiO on ITO. Therefore, spin speed should be arranged to obtain optimum thickness of layers while coating NiO, perovskite and ZnO.

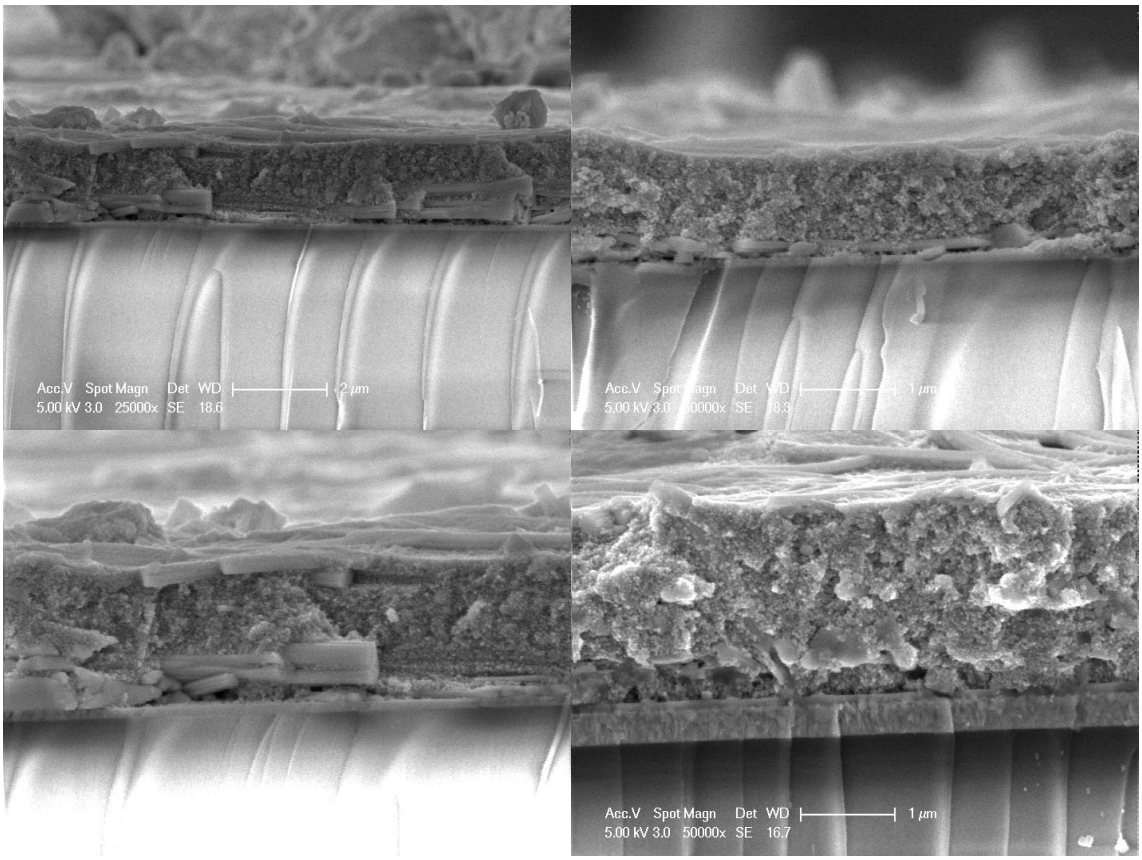

Figure 4.7. Cross-sectional SEM image of NiO/$CH_3NH_3PbI_3$/ZnO/Al structure.

Perovskite solar cells with different cell designs and HTL thicknesses demonstrated various results. The cells with best performances are given in Table 4.2 with their electrical

characterizations and active area values. The open circuit voltage and short circuit current density were obtained from the J-V curves of the devices. In addition, P-V curves give the maximum power point voltage and current values to be used in efficiency calculation. Figure 4.8, 4.10, 4.12, and 4.14 are the J-V curves of solar cells while Figure 4.9, 4.11, 4.13, and 4.15 demonstrate the power curve of the perovskite solar cells.

The first cell which have NiO/$MAPbI_3$/ZnO/Al configuration has the highest power conversion efficiency as 7.27×10^{-3}% which is very low with respect to literature. Open circuit voltage was obtained as 0.51 V while short circuit current was 5.21×10^{-2} mA/cm^2. You *et al.* achieved 16.1% PCE with 76 % FF and obtained 1.01 V V_{OC} and 21.0 mA/cm^2 J_{SC} with the same configuration (You *et al.*, 2015). Since the current density is poor due to inefficient perovskite formation under moisture and oxygen effect, the PCE of the cell is very low. Also, the thickness of the layers is significant parameter that effects the solar cell efficiency. The thickness of NiO, perovskite and ZnO layers are larger than the literature values causing decreased efficiency due to high electrical resistance. Moreover, the deposition methods of NiO and ZnO nanoparticles are also another consideration point. NiO layer was produced by applying NiO solution on ITO substrate and annealing. Because it was difficult to cover ITO surface with NiO, the procedure was repeated several times. However, this resulted in increased thickness of NiO decreasing the device performance. Also, ZnO nanoparticles interacted with perovskite affecting the bonds of the perovskite structure. In addition, ZnO was dispersed in butyl acetate which partially harms the perovskite structure. Thus, the solar performance could decrease. Furthermore, the device that was fabricated by You *et al.* Al had back contact which was thermally evaporated on the ZnO surface, but Al was used as a back electrode in this study. While the thermally evaporated Al layer was 30 nm, the thickness of Al tape was 0.081 mm. The large film thickness caused decreased efficiency of solar cells. In contrast, Shao *et al.* used metal tape as back electrode of the solar cell with efficiency of 12.7% indicating that the thickness of the metal tape was not the major effect of the poor performance of the solar cells (Shao *et al.*, 2015). J-V and power curve of this structure is shown in Figure 4.8 and 4.9 and electrical characterizations are listed in Table 4.2.

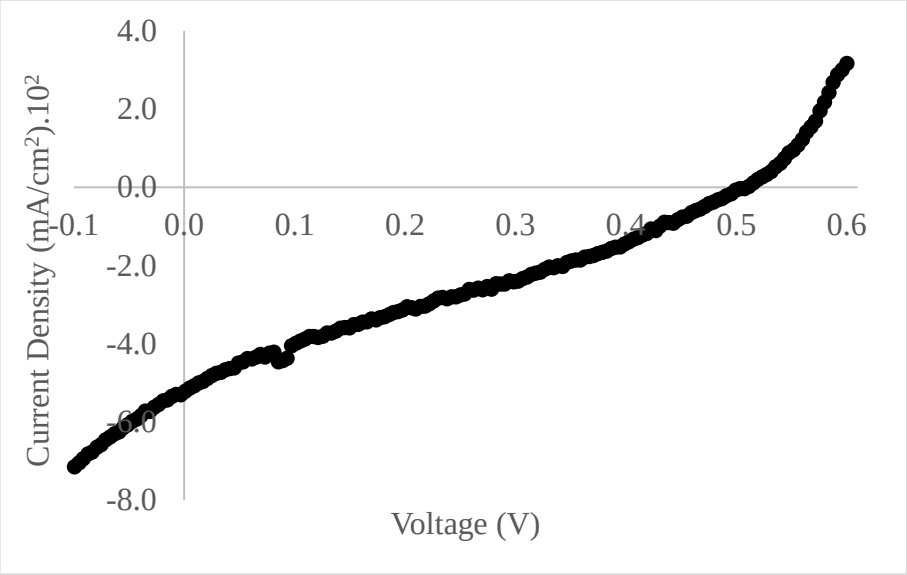

Figure 4.8. J-V curve of $NiO/CH_3NH_3PbI_3/ZnO/Al$ structure with 4 layers of NiO.

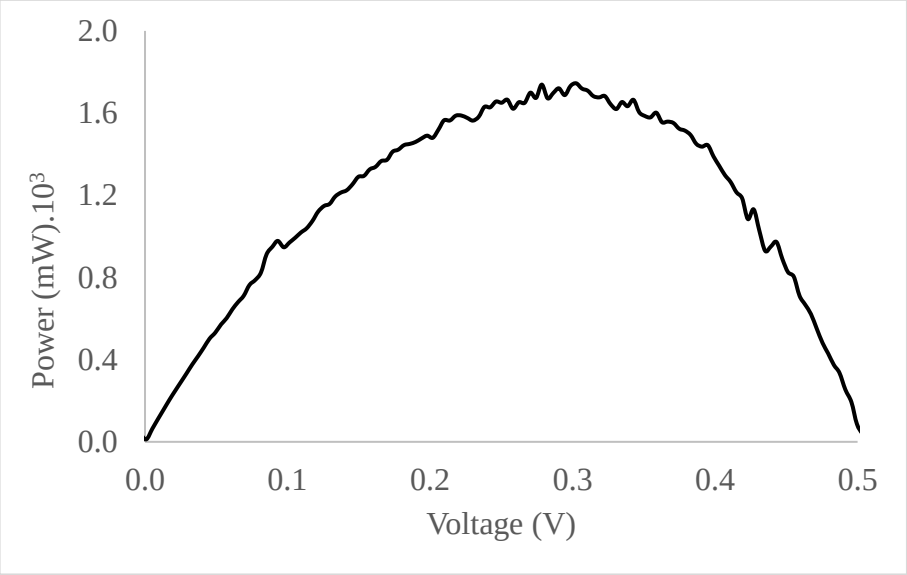

Figure 4.9. P-V curve of $NiO/CH_3NH_3PbI_3/ZnO/Al$ structure with 4 layers of NiO.

Perovskite solar cell with $NiO/MAPbI_3/ZnO/Cu$ structure showing 5.25×10^{-4} % power conversion efficiency was fabricated applying 4 layers of NiO. The back electrode of this device is Cu tape which was attached to ZnO surface. This device achieved 20.8 % FF, 0.26 V V_{OC} and 9.81×10^{-3} mA/cm^2 J_{SC}. The conductivity of Cu is higher than Al and active area of Cu is smaller than Al, but the Cu tape containing cell showed lower performance than the former cell. In contrast, the performance of the Cu taped cell should have been

greater than the Al tape containing device. J-V and power curve of the solar cell are displayed in Figure 4.10 and 4.11, respectively and characterization results are given in Table 4.2.

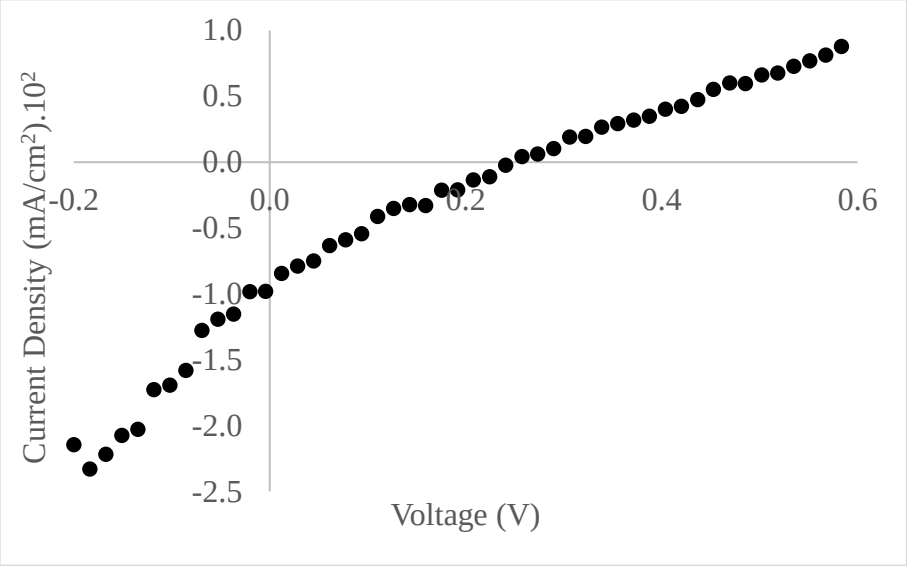

Figure 4.10. J-V curve of $NiO/CH_3NH_3PbI_3/ZnO/Cu$ structure with 4 layers of NiO.

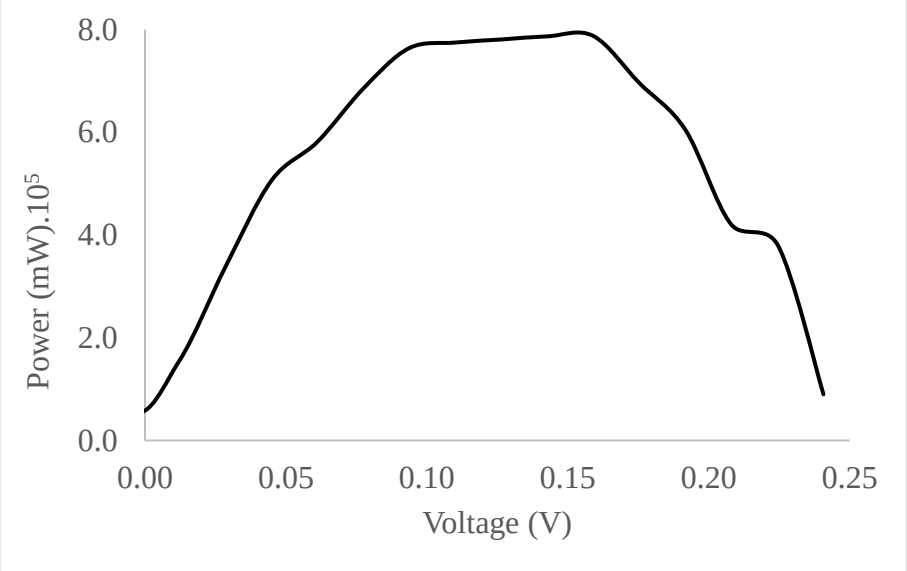

Figure 4.11. P-V curve of $NiO/CH_3NH_3PbI_3/ZnO/Cu$ structure with 4 layers of NiO.

Perovskite solar cell with $NiO/MAPbI_3/ZnO/Au$ structure displays 9.18×10^{-5}% PCE consists of 4 layers of NiO. Au was sputtered on the surface of ZnO to be used as cathode of the cell. This solar cell produced 0.08 V V_{OC} and 2.22×10^{-3} mA/cm^2 J_{SC} while FF was 53.2%. Although FF is quite high and current density has the similar magnitude of current with the previous cell, open circuit voltage is very low. Due to decreased amount of voltage,

the cell performance becomes poor. The sputtering may harm ZnO particles, and the sputtered Au may diffuse into perovskite damaging the structure. As a result, it can be said that sputtering method is not suitable for perovskite solar cell fabrication. The J-V and power curves of perovskite solar cell are showed in Figure 4.12 and 4.13, respectively and characterization results are listed in Table 4.2.

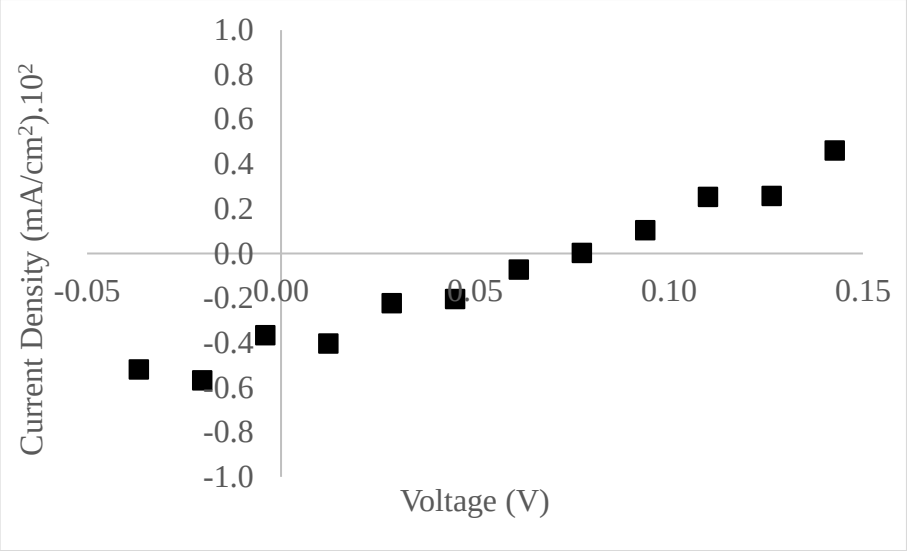

Figure 4.12. J-V curve of NiO/$CH_3NH_3PbI_3$/ZnO/Au structure with 4 layers of NiO.

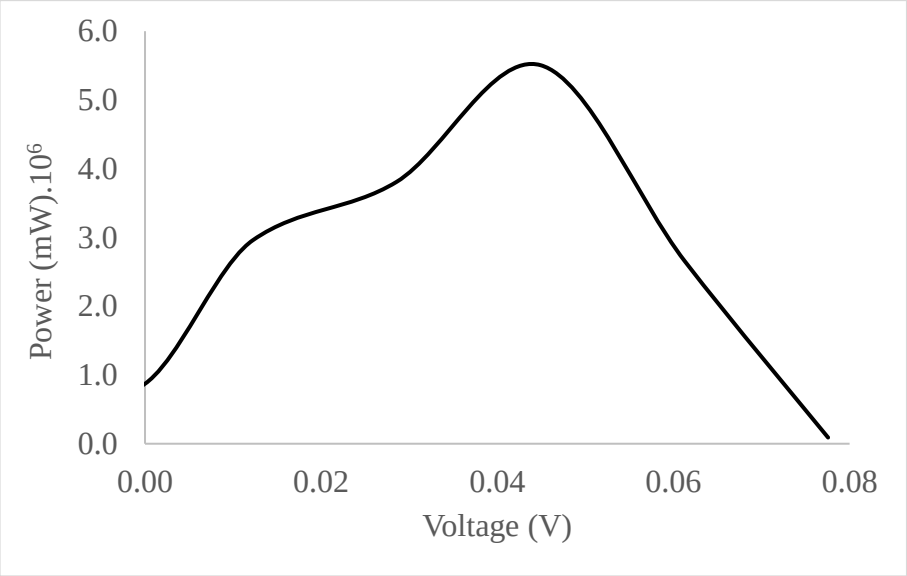

Figure 4.13. P-V curve of NiO/$CH_3NH_3PbI_3$/ZnO/Au structure with 4 layers of NiO.

The perovskite solar cell with NiO/$CH_3NH_3PbI_3$/ZnO/Al configuration fabricated by applying 6 layers of NiO. The most significant difference between this cell and the solar cell with the best performance is the NiO layer thicknesses. Due to increase in the thickness, open circuit voltage diminished while current density stayed at a similar value. Overall, the power conversion efficiency slightly dropped to 5.47×10^{-3}% while FF increases up to 35.1%. Open circuit voltage became 0.31V and short current density of perovskite solar cell was 4.96×10^{-2} mA/cm^2. J-V and P-V curves are demonstrated in Figure 4.14 and 4.15, respectively. Electrical properties of the PSC are shown in Table 4.2.

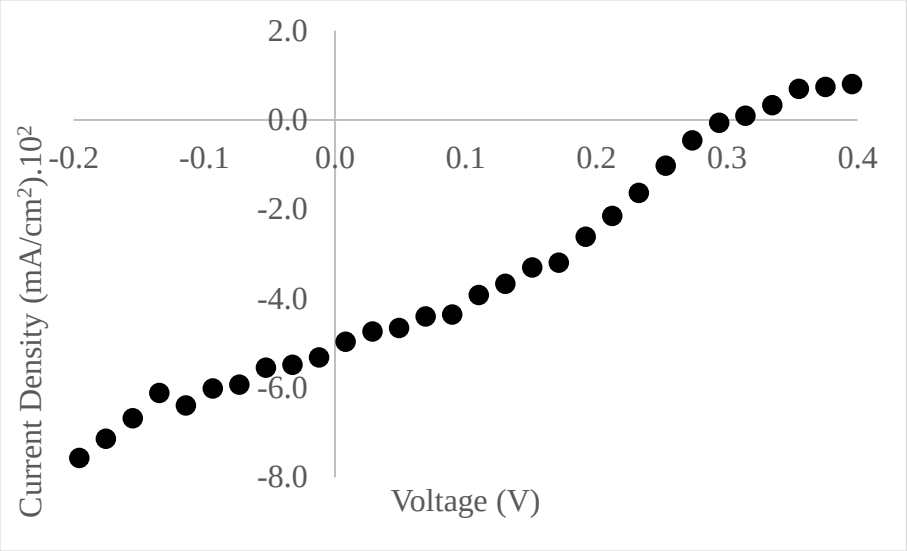

Figure 4.14. J-V curve of NiO/$CH_3NH_3PbI_3$/ZnO/Al structure with 6 layers of NiO.

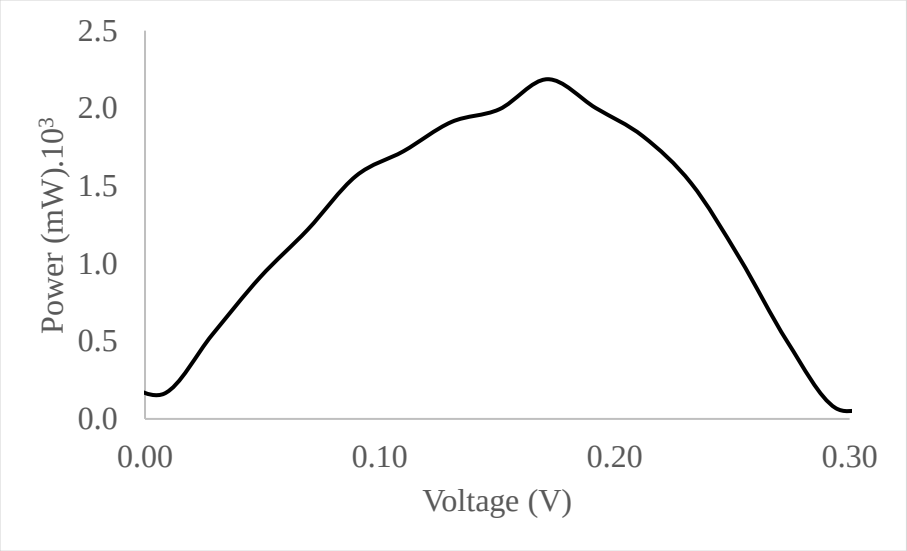

Figure 4.15. P-V curve of NiO/$CH_3NH_3PbI_3$/ZnO/Al structure with 6 layers of NiO.

Table 4.2. Performances of ZnO as ETL devices.

Device Configuration	PCE (%)	FF (%)	J_{SC} (mA/cm^2)	V_{OC} (V)	Active Area (cm^2)	NiO layers
NiO/Perovskite/ZnO/Al	7.27×10^{-3}	27.3	5.21×10^{-2}	0.51	0.24	4
NiO/Perovskite/ZnO/Cu	5.25×10^{-4}	20.8	9.81×10^{-3}	0.26	0.15	4
NiO/Perovskite/ZnO/Au	9.18×10^{-5}	53.2	2.22×10^{-3}	0.08	0.06	4
NiO/Perovskite/ZnO/Al	5.47×10^{-3}	35.1	4.96×10^{-2}	0.31	0.40	6

4.4. NiO as HTL and Ionic Liquid as ETL Structure

Inverted planar solar cell configuration was designed using NiO as hole transport material and an ionic liquid as electron transport material. The ionic liquid used was 1-Ethyl-3-methylimidazolium bis (trifluoromethylsulfonyl) imide, which is in the form of molten salt at room temperature. It is a non-volatile, highly ionic and electrically conductive material. Due to convenient properties of ionic liquids, they were used as electron transport material in perovskite solar cell fabrication.

The procedure of perovskite solar cell production was the same with the ZnO ETL structure. Ionic liquid containing solar cell was generated with applying 4 layers of NiO on etched ITO substrate. Then, perovskite layer was created by using sequential deposition method. The key step was the addition of electron transport material which was the ionic liquid. 1-Ethyl-3-methylimidazolium bis (trifluoromethylsulfonyl) imide was coated on perovskite material creating a gel-like layer. In the first trials, annealing was applied after ionic liquid coating. However, annealing induced degradation of perovskite affecting the chemical structure. Therefore, annealing was not applied to be able to obtain efficient solar cell. The solar cell was completed with Al tape attachment on the ionic liquid surface.

Perovskite solar cell with NiO/$MAPbI_3$/IL/Al structure demonstrated 1.07×10^{-3}% power conversion efficiency with 17.2% FF. Also, this structure produced 0.27V open circuit voltage and 2.28×10^{-2} mA/cm^2 short circuit current density under illumination. The results of this structure were favorable when it is compared to ZnO containing solar cells. This indicates that usage of an ionic liquid as an electron transport material was a proper

application that can be developed in future. J-V and P-V curves of the solar cell are given in Figure 4.16 and 4.17, respectively and electrical characterization results are listed in Table 4.3.

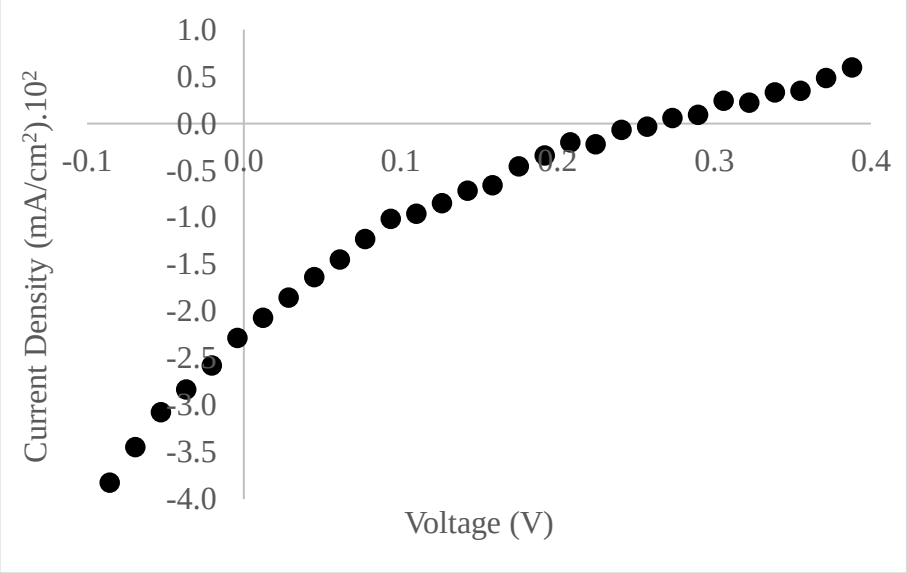

Figure 4.16. J-V curve of NiO/$CH_3NH_3PbI_3$/IL/Al structure with 4 layers of NiO.

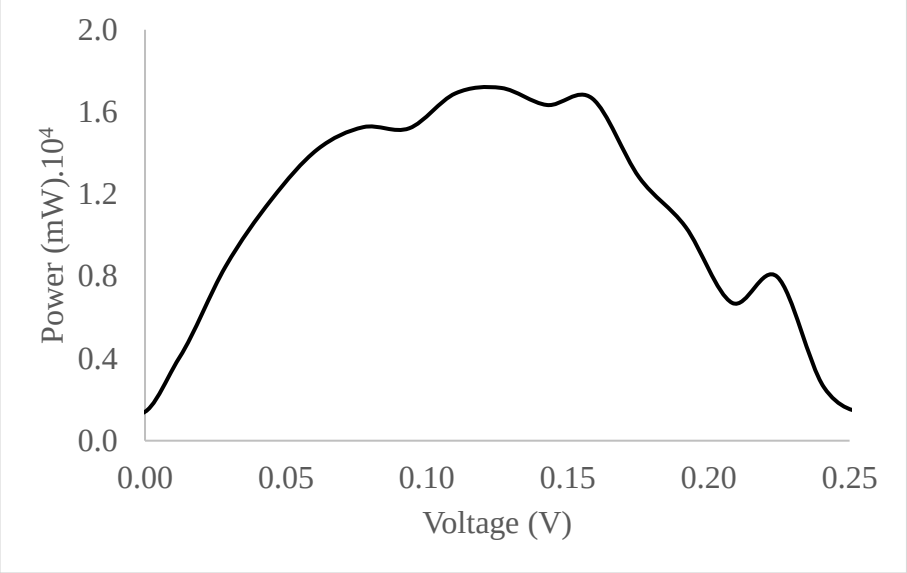

Figure 4.17. P-V curve of NiO/$CH_3NH_3PbI_3$/IL/Al structure with 4 layers of NiO.

Table 4.3. Performances of Ionic Liquid as ETL devices.

Device Configuration	PCE (%)	FF (%)	J_{SC} (mA/cm^2)	V_{OC} (V)	Active Area (cm^2)	NiO layers
NiO/Perovskite/IL/Al	1.07×10^{-3}	17.2	2.28×10^{-2}	0.27	0.16	4

4.5. NiO as HTL and without ETL Structure

Perovskite solar cells usually fabricated by using a hole transport layer, an electron transport layer and perovskite layer in between them. Beside this configuration, ETL-free and HTL-free devices are also generated depending on the electron-hole extraction ability of perovskite material. Perovskite is a crystal structure with high ionic properties providing efficient conductivity. Thus, ETL-free and HTL-free devices can produce electricity with a small efficiency drop.

ETL-free structure was performed during experiments by just extracting the electron transport layer from the configuration. According to the previous studies, it was known that ETL-free devices had low performance compared with the other devices. However, it was conducted since ZnO was damaging the perovskite structure. In order to observe the effect of ZnO on perovskite material, ETL-free cells were fabricated. It was seen that efficient perovskite layer could be synthesized in spite of moisture exposure, but ZnO nanoparticles harmed the perovskite structure during the annealing process.

In Figure 4.18, SEM image of ETL-free perovskite solar cell is displayed. When the image is examined, there is a melt-like structure in addition to crystals. Because of humidity, perovskite was degrading, and crystal structure was beginning to disappear. This condition was a drawback of the ETL-free structure. The ETL was protecting the perovskite structure from humidity and oxygen exposure. When there was no ETL to prevent air diffusion, perovskite can easily degrade lowering the device performance.

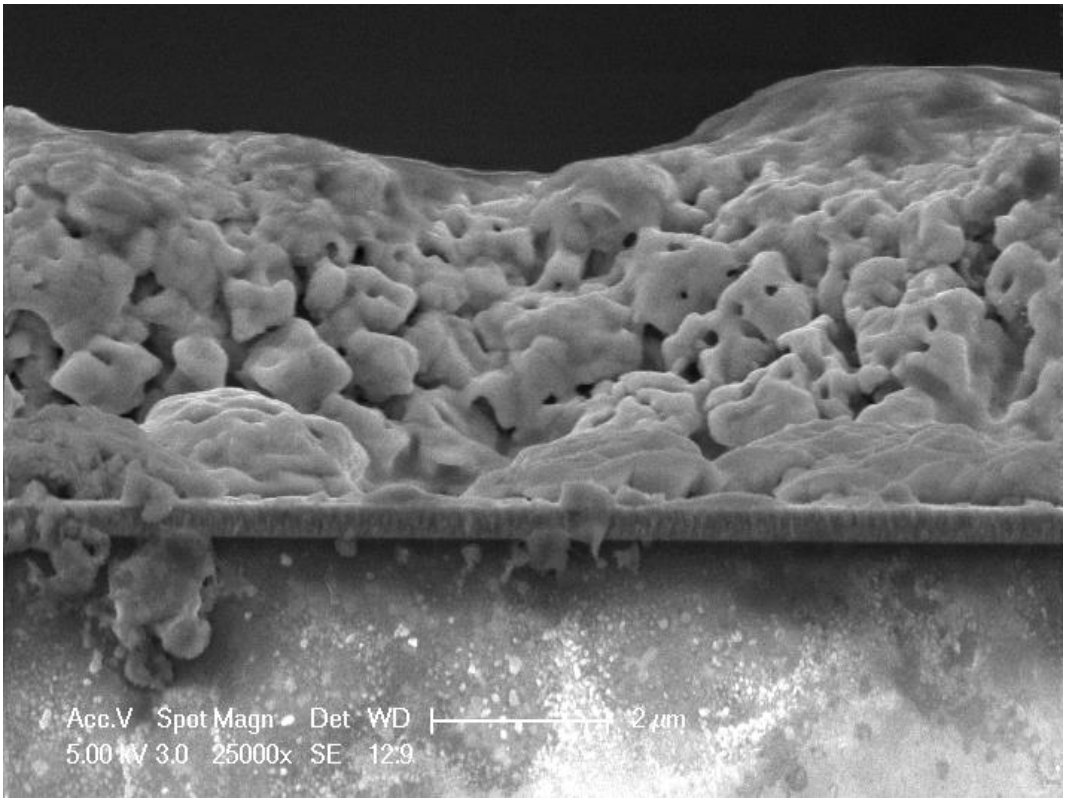

Figure 4.18. SEM image of perovskite degradation.

Various ETL-free solar cells were generated. First, NiO was coated on ITO substrates with varied thicknesses. 4, 8, and 10 layers of NiO was used as hole transporting material. The perovskite was coated on NiO by both one step and two step deposition methods in air, but only sequentially deposited cells could work. Then, Al tape was directly added to perovskite surface. Three different ETL-free solar cells were prepared with varying NiO thicknesses. The PCE of the cells were 2.86×10^{-3}%, 3.86×10^{-4}%, and 8.14×10^{-4}%, respectively. According to the results, it can be said that as thickness of NiO increases, the efficiency of the device decreases. However, the PCE of perovskite solar cell with 8 layers of NiO was lower than the cell with 10 NiO layers. This indicates that not only the thickness influences the performance but also active area of the device is effective. In addition, the Al tape attached to surface may not be pasted properly. If there was air or gap between the top layer surface and the tape, it will decrease the conductivity reducing the performance of the cell. Therefore, roll to roll method was applied, but it was not sufficient for the complete adhesion. Before rolling, the tape was heated to provide better adhesion.

ETL-free PSCs containing Al tape as cathode with 4,8, and 10 layers of NiO produced 6.19×10^{-2}, 5.75×10^{-3}, and 1.26×10^{-2}mA/cm^2 short circuit current density and 0.24V, 0.29V and 0.18 V open circuit voltage, respectively. The fill factor values were 19.2%, 23.1% and 36.1%. J-V curves are shown in Figure 4.19, 4.21, and 4.23 while power curves are given in Figure 4.20, 4.22, and 4.24. The electrical characterization values are listed in Table 4.4.

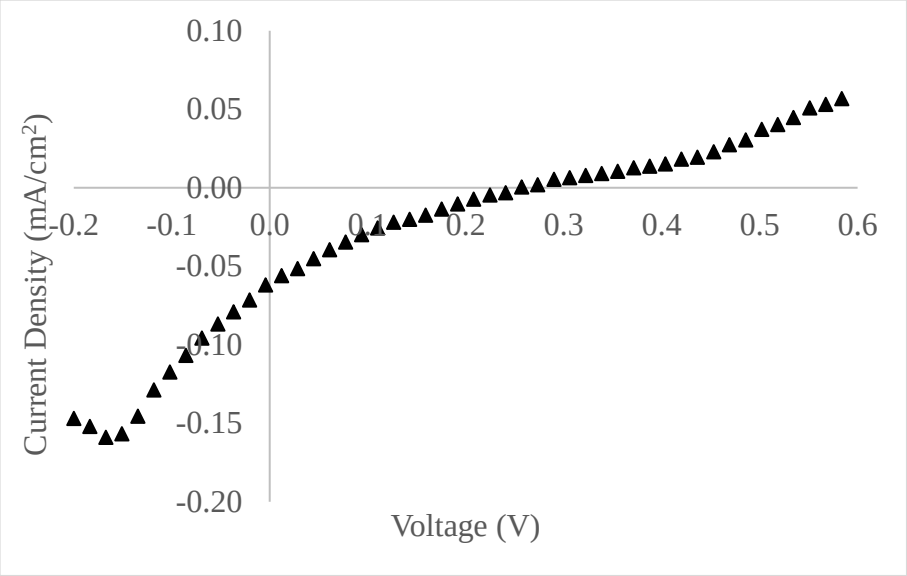

Figure 4.19. J-V curve of NiO/$CH_3NH_3PbI_3$/Al structure with 4 layers of NiO.

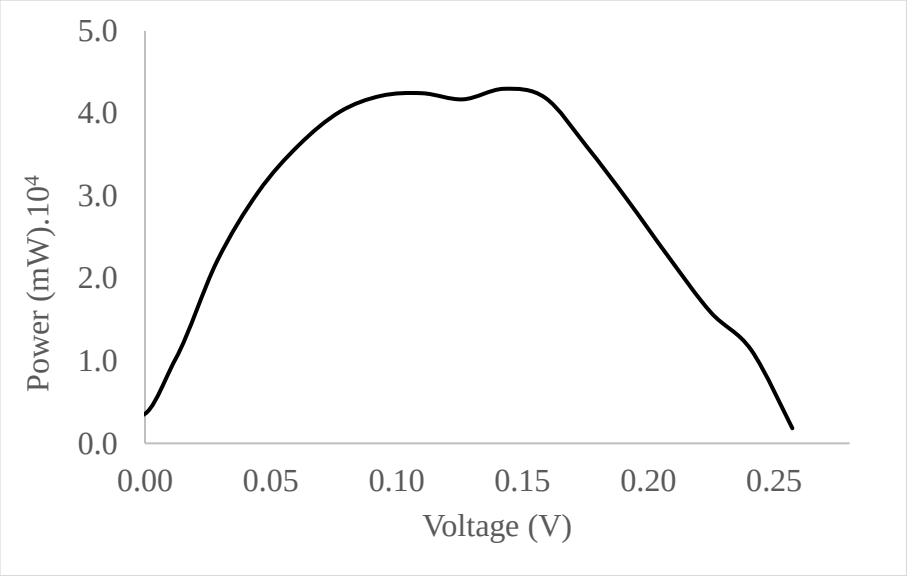

Figure 4.20. P-V curve of NiO/$CH_3NH_3PbI_3$/Al structure with 4 layers of NiO.

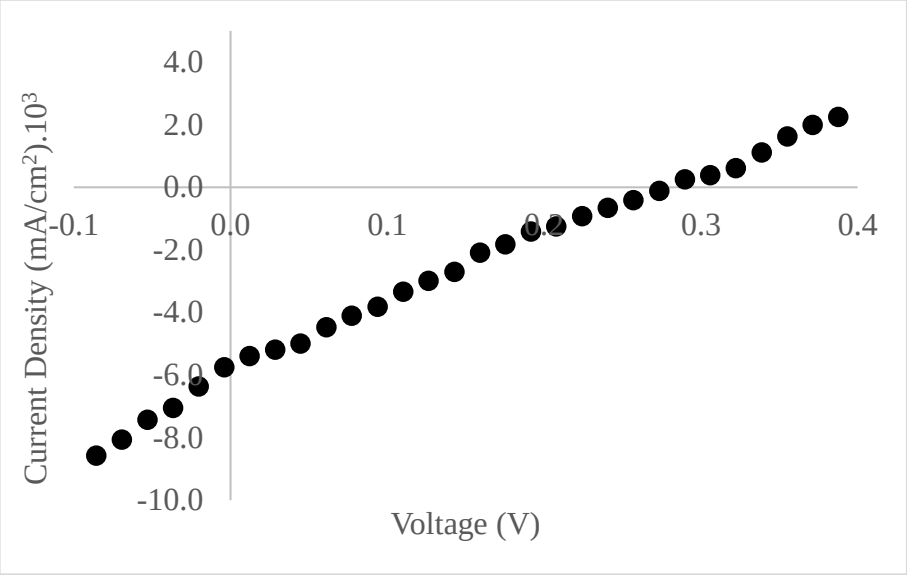

Figure 4.21. J-V curve of $NiO/CH_3NH_3PbI_3/Al$ structure with 8 layers of NiO.

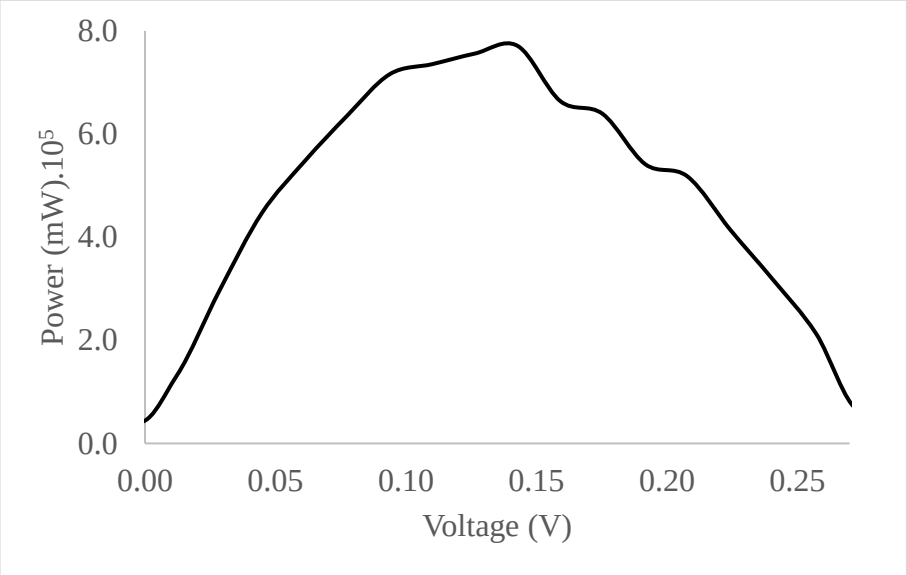

Figure 4.22. P-V curve of $NiO/CH_3NH_3PbI_3/Al$ structure with 8 layers of NiO.

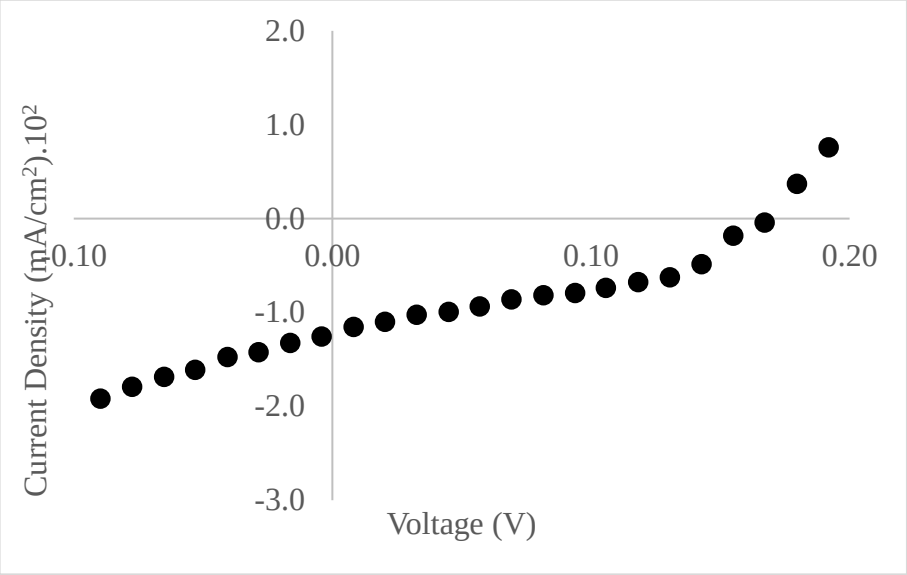

Figure 4.23. J-V curve of $NiO/CH_3NH_3PbI_3/Al$ structure with 10 layers of NiO.

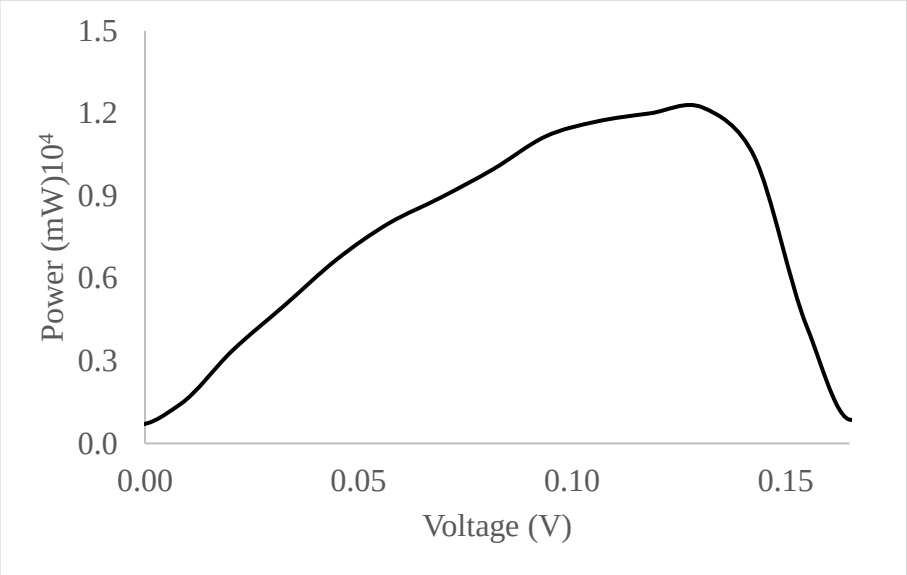

Figure 4.24. P-V curve of $NiO/CH_3NH_3PbI_3/Al$ structure with 10 layers of NiO.

ETL-free perovskite solar cell containing Cu tape electrode was produced applying 4 layers of NiO. This configuration caused the lowest efficiency among ETL-free devices performed. Perovskite solar cell with NiO/Perovskite/Cu structure showed 2.88×10^{-4}% power conversion efficiency with 52.2% FF. In addition, this device produced 0.19V open circuit voltage and 2.87×10^{-3} mA/cm^2 short circuit current density under light illumination. J-V and P-V curves of the structure is demonstrated in Figure 4.25 and 4.26 respectively. And, characterization values are given in Table 4.4.

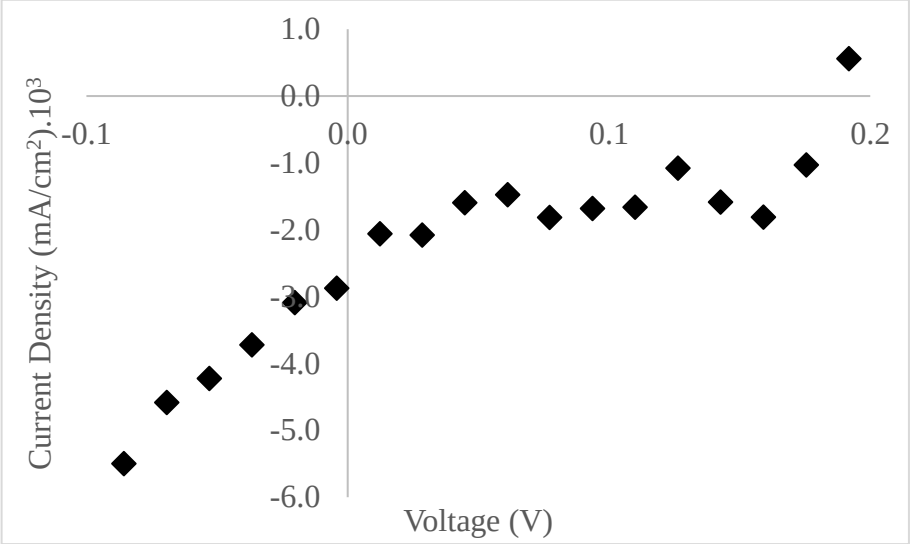

Figure 4.25. J-V curve of $NiO/CH_3NH_3PbI_3/Cu$ structure with 4 layers of NiO.

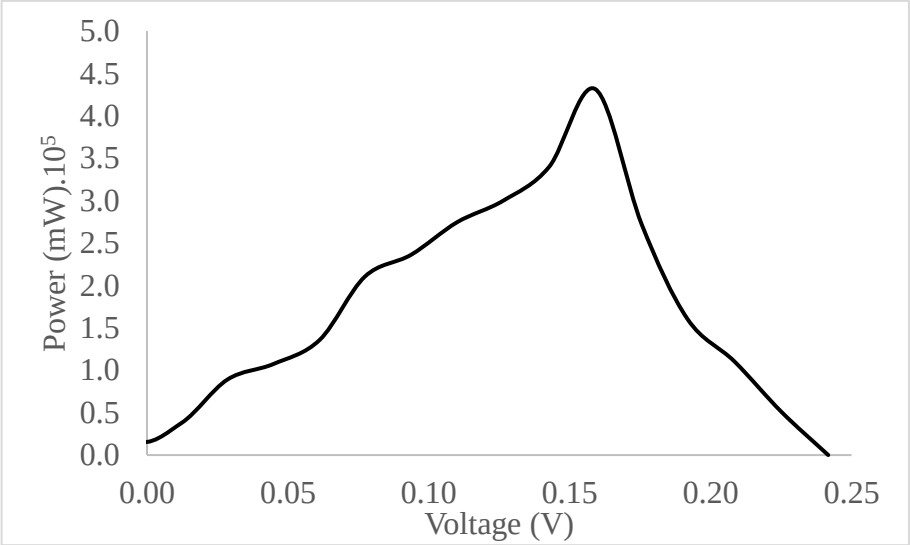

Figure 4.26. P-V curve of $NiO/CH_3NH_3PbI_3/Cu$ structure with 4 layers of NiO.

Table 4.4. Performances of ETL-free devices.

Device Configuration	PCE (%)	FF (%)	J_{SC} (mA/cm^2)	V_{OC} (V)	Active Area (cm^2)	NiO layers
NiO/Perovskite/Al	2.86×10^{-3}	19.2	6.19×10^{-2}	0.24	0.15	4
NiO/Perovskite/Al	3.86×10^{-4}	23.1	5.75×10^{-3}	0.29	0.20	8
NiO/Perovskite/Al	8.14×10^{-4}	36.1	1.26×10^{-2}	0.18	0.15	10
NiO/Perovskite/Cu	2.88×10^{-4}	52.2	2.87×10^{-3}	0.19	0.15	4

4.6. Overall Results

All perovskite solar cells fabricated in this study are listed in Table 4.5 with their structure details, deposition methods and electrical characterizations.

Table 4.5. Device Configurations and Performances.

Device Configuration	Perovskite Deposition Method	NiO layers	Photovoltaic Parameters			
			V_{OC} (V)	J_{SC} (mA/cm^2)	FF (%)	PCE (%)
TiO_2 / $CH_3NH_3PbI_3$ / PCBM / Al	1-Step	-	0.11	0.0015	16.2	2.61×10^{-5}
TiO_2 / $CH_3NH_3PbI_3$ / PCBM/ Cu	1-Step	-	0.14	0.0039	21.2	1.21×10^{-4}
TiO_2 / $CH_3NH_3PbI_3$ / ZnO / Al	2-Step	-	-	-	-	N/A
NiO / $CH_3NH_3PbI_3$ / ZnO / Al	2-Step	4	0.51	0.0521	27.3	7.27×10^{-3}
NiO / $CH_3NH_3PbI_3$ / ZnO / Al	2-Step	5	-	-	-	N/A
NiO / $CH_3NH_3PbI_3$ / ZnO / Al	2-Step	6	0.31	0.0496	35.1	5.47×10^{-3}
NiO / $CH_3NH_3PbI_3$ / ZnO / Al	2-Step	8	-	-	-	N/A
NiO / $CH_3NH_3PbI_3$ / ZnO / Al	2-Step	10	-	-	-	N/A
NiO / $CH_3NH_3PbI_3$ / ZnO / Cu	2-Step	4	0.26	0.0098	20.8	5.25×10^{-4}
NiO / $CH_3NH_3PbI_3$ / ZnO / Au	2-Step	4	0.08	0.0022	53.2	9.18×10^{-5}
NiO / $CH_3NH_3PbI_3$ / ZnO / Al	1-Step	6	-	-	-	N/A
NiO / $CH_3NH_3PbI_3$ / ZnO / Al	1-Step	10	-	-	-	N/A
NiO / $CH_3NH_3PbI_3$ / IL / Al	2-Step	4	0.27	0.0228	17.2	1.07×10^{-3}
NiO / $CH_3NH_3PbI_3$ / IL / Cu	2-Step	4	-	-	-	N/A
NiO / $CH_3NH_3PbI_3$ / Al	2-Step	4	0.24	0.0619	19.2	2.86×10^{-3}
NiO / $CH_3NH_3PbI_3$ / Al	2-Step	5	-	-	-	N/A
NiO / $CH_3NH_3PbI_3$ / Al	2-Step	8	0.29	0.0057	23.1	3.86×10^{-4}
NiO / $CH_3NH_3PbI_3$ / Al	2-Step	10	0.18	0.0126	36.1	8.14×10^{-4}
NiO / $CH_3NH_3PbI_3$ / Cu	2-Step	4	0.19	0.0029	52.2	2.88×10^{-4}
NiO / $CH_3NH_3PbI_3$ / Al	1-Step	4	-	-	-	N/A
NiO / $CH_3NH_3PbI_3$ / Al	1-Step	5	-	-	-	N/A

4.7. Challenges

Methylammonium lead iodide perovskite solar cells were fabricated in this study applying many steps that may affect the film quality and the performance of the solar cells. While the cells were undergoing various operations, several problems occurred.

First, it was not easy to keep the substrate clean. Both dust and unused chemicals stick to the glass. In order to coat the desired areas of the glass, non-coated places were covered with plastic or paper tape. However, when the tapes were removed, they left some sticky material on the surface. Moreover, if the sample was annealed, it would be very difficult to remove the remaining adhesive.

Another problem was the perovskite deposition in air. Even the same procedure was applied at the same time, two substrates could result in distinct perovskite coverage and diverse performances. Both humidity and oxygen in air are harmful for the perovskite material. Therefore, most of the perovskite synthesis was conducted in glovebox with nitrogen environment. In addition, while producing perovskite layer by dropping the MAI on PbI_2 coverage, the droplet caused non-uniform distribution of MAI on the surface.

Furthermore, the addition of conductive tape was a crucial step for the perovskite solar cells. The conductive tape should be attached to the surface avoiding any dust, air or gap between the tape and the surface. Thus, rolling was applied. However, it was not enough to obtain complete adhesion. So, fabricated cell was heated before placing the tape, but further heating may cause problem on perovskite structure. On the other hand, short circuit should be avoided during the cell fabrication. So, the place of the tape was an important consideration. The conductive tape should not touch the ITO or FTO layer, which will lead short circuit along the cell. Moreover, thickness of metal tapes is greater than that of metals which are thermally evaporated on the cell, which causes poor performance of the device.

Lastly, the perovskite material is not stable under ambient conditions. The perovskite degrades so fast that fabricated cell should be characterized immediately after completing the cell production, or the cell should be kept under nitrogen environment to be able to get high performance.

5. CONCLUSIONS AND RECOMMENDATIONS

5.1. Conclusions

The object of this thesis was to fabricate organolead halide perovskite solar cells by using inexpensive and easily synthesizable materials applying processes which are appropriate for large scale production.

The best performing device had configuration with 4 layers of NiO coated on ITO substrate as hole transport material, methylammonium iodide perovskite which was produced by sequential deposition method, ZnO as electron transport material, and Al tape back electrode.

The thickness of charge transport layers directly affects the performance of the solar cell; hence optimum thickness of NiO and ZnO should be provided by adjusting spin speed.

TiO_2 based solar cells showed the lowest efficiencies due to inappropriate charge transport material selection and weak perovskite film formation which was produced by one-step deposition method.

Ionic liquid, 1-Ethyl-3-methylimidazolium bis (trifluoromethylsulfonyl) imide worked efficiently as electron transport material in inverted planar devices.

ETL-free perovskite solar cells displayed good performance with a small decrease in the power conversion efficiency with respect to ZnO ETL cells.

Back electrode addition by metal sputtering is not a convenient method to be used in perovskite solar cell fabrication, since metal ions damaged the perovskite structure.

Moisture and oxygen in air harmed the materials; therefore, the experiments should be carried out in nitrogen glovebox which provides a controlled environment.

5.2. Recommendations

The recommendations for the development of this study and the future work can be expressed as:

- Methylammonium iodide was synthesized and deposited under ambient air conditions. It should be produced under nitrogen environment.
- While synthesizing the perovskite under ambient air, the humidity of environment should be controlled and kept at a certain level.
- In addition to methylammonium iodide, mixed halide perovskite can be generated to increase stability and performance of the device.
- Dip coating method can be applied to coat the glass substrate with perovskite materials.
- Instead of DMF, DMSO and GBL can be used to prepare perovskite precursor solutions. Also, solvent mixtures can be used to obtain efficient perovskite film.
- In order to accelerate the evaporation of solvents, non-dissolving solvents such as toluene and chlorobenzene may be dropped on perovskite surface during spin coating process to obtain high quality perovskite film generation.

REFERENCES

Aharon, S., B. E. Cohen and L. Etgar, 2014, "Hybrid Lead Halide Iodide and Lead Halide Bromide in Efficient Hole Conductor Free Perovskite Solar Cell", *The Journal of Physical Chemistry C*, Vol. 118, pp. 17160–17165.

Asghar, M.I., J. Zhang, H. Wang, and P. D. Lund, 2017, "Device stability of perovskite solar cells – A review", *Renewable and Sustainable Energy Reviews*, Vol. 77, pp. 131-146.

Bakr, Z. H., Q. Wali, A. Fakharuddin, L. Schmidt-Mende, T. M. Brown, and R. Jose, 2017, "Advances in hole transport materials engineering for stable and efficient perovskite solar cells", *Nano Energy*, Vol. 34, pp. 271-305.

Becquerel, A. E., 1839, "Recherches sur les effets de la radiation chimique de la lumiere solaire au moyen des courants electriques.", *Comptes Rendus de L´Academie des Sciences*, Vol. 9, pp. 145-149.

Bella, F., 2015, "Polymer electrolytes and perovskites: lights and shadows in photovoltaic devices", *Electrochimica Acta*, Vol. 175, pp. 151–161.

Burschka, J., N. Pellet, S. J. Moon, R. Humphry-Baker, P. Gao, M. K. Nazeeruddin, and M. Grätzel, 2013, "Sequential deposition as a route to high-performance perovskite-sensitized solar cells.", *Nature*, Vol. 499, pp. 316-319.

Chang, J., H. Zhu, J. Xiao, F. H. Isikgor, Z. Lin, Y. Hao, K. Zeng, Q.-H. Xu, and J. Ouyang, 2016, "Enhancing the planar heterojunction perovskite solar cell performance through tuning the precursor ratio", *Journal of Materials Chemistry A*, Vol. 4, pp. 7943-7949.

Chapin, D. M., C. S. Fuller and G. L. Pearson, 1954, "A New Silicon p-n Junction Photocell for Converting Solar Radiation into Electrical Power", *Journal of Applied Physics*, Vol. 25, pp. 676-677.

Chen, Q., H. Zhou, Z. Hong, S. Luo, H. S. Duan, H. H. Wang, Y. Liu, G. Li, Y. Yang, 2013, "Planar Heterojunction Perovskite Solar Cells via Vapor-Assisted Solution Process", *Journal of the American Chemical Society*, Vol. 136, pp. 622-625.

Chen, Q., N. De Marco, Y. (M.) Yang, T. B. Song, C. C. Chen, H. Zhao, Z. Hong, H. Zhou, Y. Yang, 2015, "Under the spotlight: The organic-inorganic hybrid halide perovskite for optoelectronic applications", *Nano Today*, Vol. 10, pp. 355-396.

Chen, Z., G. Yang, X. Zheng, H. Lei, C. Chen, J. Ma, H. Wang, and G. Fang, 2017, "Bulk heterojunction perovskite solar cells based on room temperature deposited hole blocking layer: Suppressed hysteresis and flexible photovoltaic application", *Journal of Power Sources*, Vol. 351, pp. 123-129.

Chiang, C. H., Z. L. Tseng, and C. G. Wu, 2014, "Planar heterojunction perovskite/$PC_{71}BM$ solar cells with enhanced open-circuit voltage via a (2/1)-step spin-coating process", *Journal of Materials Chemistry A*, Vol. 2, pp. 15897-15903.

Ciro, J., R. Betancur, S. Mesa, and F. Jaramillo, 2017, "High performance perovskite solar cells fabricated under high relative humidity conditions", *Solar Energy Materials & Solar Cells*, Vol. 163, pp. 38-42.

Cohen, B. E., S. Aharon, A. Dymshits, and L. Etgar, 2015, "Impact of Antisolvent Treatment on Carrier Density in Efficient Hole-Conductor-Free Perovskite-Based Solar Cells", *The Journal of Physical Chemistry C*, Vol. 120, pp. 142-147.

Docampo, P., J. M. Ball, M. Darwich, G. E. Eperon, and H. J. Snaith, 2013, "Efficient organometal trihalide perovskite planar-heterojunction solar cells on flexible polymer substrates.", *Nature Communications*, Vol. 4, p. 2461.

Eperon, G. E., V. M. Burlakov, P. Docampo, A. Goriely, and H. J. Snaith, 2014, "Morphological Control for High Performance, Solution-Processed Planar Heterojunction Perovskite Solar Cells", *Advanced Functional Materials*, Vol. 24, pp. 151-157.

Etgar, L., P. Gao, Z. Xue, Q. Peng, A. K. Chandiran, B. Liu, Md. K. Nazeeruddin, and M. Grätzel, 2012, "Mesoscopic $CH_3NH_3PbI_3/TiO_2$ Heterojunction Solar Cells", *Journal of the American Chemical Society*, Vol. 134, pp. 17396-17399.

Gamliel, S., A. Dymshits, S. Aharon, E. Terkieltaub, and L. Etgar, 2015, "Micrometer Sized Perovskite Crystals in Planar Hole Conductor Free Solar Cells", *The Journal of Physical Chemistry C*, Vol. 119, pp. 19722-19728.

Giacomo, F., S. Razza, F. Matteocci, A. D'Epifanio, S. Licoccia, T. M. Brown, A. Di Carlo, 2014, "High efficiency $CH_3NH_3PbI_{(3-x)}Cl_x$ perovskite solar cells with poly(3-hexylthiophene) hole transport layer", *Journal of Power Sources*, Vol. 251, pp. 152-156.

Grätzel, C. and S. M. Zakeeruddin, 2013, "Recent trends in mesoscopic solar cells based on molecular and nanopigment light harvesters", *Materials Today*, Vol. 16, pp. 11-18.

Green, M. A., 2005, "Silicon photovoltaicmodules: a brief history of the first 50 years", *Progress in Photovoltaics: Research and Applications*, Vol. 13, pp. 447–455.

Han, G., S. Zhang, P. P. Boix, L. H. Wong, L. Sun, and S.-Y. Lien, 2017, "Towards high efficiency thin film solar cells", *Progress in Materials Science*, Vol. 87, pp. 246-291.

Hatamvand, M., S. A. Mirjalili, M. Sharzehee, A. Behjat, M. Jabbari, and M. Skrifvars, 2017, "Fabrication parameters of low-temperature ZnO-based hole-transport-free perovskite solar cells", *Optik*, Vol. 140, pp. 443-450.

Huang, L., C. Li, X. Sun, R. Xu, Y. Du, J. Ni, H. Cai, J. Li, Z. Hu, and J. Zhang, 2016, "Efficient and hysteresis-less pseudo-planar heterojunction perovskite solar cells fabricated by a facile and solution-saving one-step dip-coating method", *Organic Electronics*, Vol. 40, pp. 13-23.

Jeng, J. Y., Y. F. Chiang, M. H. Lee, S. R. Peng, T. F. Guo, P. Chen and T. C. Wen, 2013, "$CH_3NH_3PbI_3$ perovskite/fullerene planar-heterojunction hybrid solar cells", *Advanced Materials*, Vol. 25, pp. 3727.

Jeon, Y., S. Lee, R. Kang, J. Kim, J. Yeo, S. Lee, S. Kim, J. M. Yun, D. Y. Kim, 2014, "Planar heterojunction perovskite solar cells with superior reproducibility", *Scientific Reports*, Vol. 4, pp. 6953.

Jung, J. W., C. C. Chueh, and A. K-Y. Jen, 2015, "A Low-Temperature, Solution-Processable, Cu-Doped Nickel Oxide Hole-Transporting Layer via the Combustion Method for High-Performance Thin-Film Perovskite Solar Cells", *Advanced Materials*, Vol. 27, pp. 7874-7880.

Kim, H. S., C. R. Lee, J. H. Im, K. B. Lee, T. Moehl, A. Marchioro, S. J. Moon, R. Humphry-Baker, J. H. Yum, J. E. Moser, M. Gärtzel, N. G. Park, 2012, "Lead iodide perovskite sensitized all-solid-state submicron thin film mesoscopic solar cell with efficiency exceeding 9%", *Scientific Reports*, Vol. 2, p. 591.

Kojima, A., K. Teshima, Y. Shirai and T. Miyasaka, 2009, "Organometal Halide Perovskites as Visible-Light Sensitizers for Photovoltaic Cells", *Journal of the American Chemical Society*, Vol. 131, pp. 6050–6051.

Krebs, F. C., 2009, "Fabrication and processing of polymer solar cells: A review of printing and coating techniques", *Solar Energy Materials & Solar Cells*, Vol. 93, pp. 394-412.

Lee, M. M., J. Teuscher, T. Miyasaka, T. N. Murakami and H. J. Snaith, 2012, "Efficient Hybrid Solar Cells Based on Meso-Superstructured Organometal Halide Perovskites", *Science*, Vol. 338, pp. 643-647.

Liu, D. and T. L. Kelly, 2014, "Perovskite solar cells with a planar heterojunction structure prepared using room-temperature solution processing techniques", *Nature Photonics*, Vol. 8, pp. 133-138.

Liu, D., J. Yang, and T. L. Kelly, 2014, "Compact Layer Free Perovskite Solar Cells with 13.5% Efficiency", *Journal of the American Chemical Society,* Vol. 136, pp. 17116-17122.

Liu, M., M. B. Johnston and H. J. Snaith, 2013, "Efficient planar heterojunction perovskite solar cells by vapour deposition", *Nature,* Vol. 501, pp. 395–398.

Liu, W., L. Li, M. Chen, X. Ding, M. Wang, G. Liu, and X. Wang, 2017, "Nucleation mechanism of $CH_3NH_3PbI_3$ with two-step method for rational design of high performance perovskite solar cells", *Journal of Alloys and Compounds,* Vol. 697, pp. 374-379.

Luo, Y., F. Meng, E. Zhao, Y. Z. Zheng, Y. Zhou, and X. Tao, 2016, "Fine control of perovskite-layered morphology and composition via sequential deposition crystallization process towards improved perovskite solar cells", *Journal of Power Sources,* Vol. 311, pp. 130-136.

Mahmud, A., N. K. Elumalai, M. B. Upama, D. Wang, K. H. Chan, M. Wright, C. Xu, F. Haque, and A. Uddin, 2017, "Low temperature processed ZnO thin film as electron transport layer for efficient perovskite solar cells", *Solar Energy Materials & Solar Cells,* Vol. 159, pp. 251-264.

Manders, J. R., S.-W. Tsang, M. J. Hartel, T.-H. Lai, S. Chen, C. M. Amb, J. R. Reynolds, and F. So, 2013, "Solution-Processed Nickel Oxide Hole Transport Layers in High Efficiency Polymer Photovoltaic Cells", *Advanced Functional Materials,* Vol. 23, pp. 2993-3001.

Marinova, N., S. Valero, and J. L. Delgado, 2017, "Organic and perovskite solar cells: Working principles, materials and interfaces", *Journal of Colloid and Interface Science,* Vol. 488, pp. 373-389.

Mehmood, U., A. Al-Ahmed, M. Afzaal, F.A. Al-Sulaiman, and M. Daud, 2017, "Recent progress and remaining challenges in organometallic halides based perovskite solar cells", *Renewable and Sustainable Energy Reviews*, Vol. 78, pp. 1-14.

National Renewable Energy Laboratory, 2017, *Photovoltaic Research*, https://www.nrel.gov/pv/assets/images/efficiency-chart.png, accessed at June 2017.

Park, M., H. J. Kim, I. Jeong, J. Lee, H. Lee, H. J. Son, D. E. Kim, M. J. Ko, 2015, "Mechanically Recoverable and Highly Efficient Perovskite Solar Cells: Investigation of Intrinsic Flexibility of Organic-Inorganic Perovskite", *Advanced Energy Materials*, Vol.5, 1501406 (pp. 1-11).

Park, N.-G., 2015, "Perovskite solar cells: an emerging photovoltaic technology", *Materials Today*, Vol. 18, pp. 65-72.

Perlin, J., 1999, *From space to earth: the story of solar electricity*, Aatec Publications, Michigan.

Petrović, M., V. Chellappan, and S. Ramakrishna, 2015, "Perovskites: Solar cells & engineering applications - materials and device developments", *Solar Energy*, Vol. 122, pp. 678-699.

Purushothaman, K. K., S. J. Antony, and G. Muralidharan, 2011, "Optical, structural and electrochromic properties of nickel oxide films produced by sol-gel technique", *Solar Energy*, Vol. 85, pp. 978-984.

Rahul, B. Bhattacharya, and Z. H. Khan, 2017, "Effect of crystal and powder of CH_3NH_3I on the $CH_3NH_3PbI_3$ based Perovskite sensitized solar cell", *Materials Research Bulletin*, Vol. 89, pp. 292-296.

Qiu, J., Y. Qiu, K. Yan, M. Zhong, C. Mu, H. Yan, and S. Yang, 2013, "All-solid-state hybrid solar cells based on a new organometal halide perovskite sensitizer and one-dimensional TiO_2 nanowire arrays.", *Nanoscale*, Vol. 5, pp. 3245-3248.

Saliba, M., T. Matsui, J. Y. Seo, K. Domanski, J. P. Correa-Baena, M. K. Nazeeruddin, S. M. Zakeeruddin, W. Tress, A. Abate, A. Hagfeldt, M. Grätzel, 2016, "Cesium-containing Triple Cation Perovskite Solar Cells: Improved Stability, Reproducibility and High Efficiency", *Energy & Environmental Science*, Vol. 9, pp. 1989-1997.

Salim, T., S. Sun, Y. Abe, A. Krishna, A. C. Grimsdale, and Y. M. Lam, 2015, "Perovskite-based solar cells: impact of morphology and device performance", *Journal of Materials Chemistry A*, Vol. 3, pp. 8943-8969.

Shao, Y., Q. Wang, Q. Dong, Y. Yuan and J. Huang, 2015, "Vacuum-free laminated top electrode with conductive tapes for scalable manufacturing of efficient perovskite solar cells, *Nano Energy*, Vol. 16, pp. 47–53.

Shi, J., J. Dong, S. Lv, Y. Xu, L. Zhu, J. Xiao, X. Xu, H. Wu, D. Li, Y. Luo, and Q. Meng, 2014, "Hole-conductor-free perovskite organic lead iodide heterojunction thin-film solar cells: High efficiency and junction property", *Applied Physics Letters*, Vol. 104, p. 63901.

Shin, S. S., E. J. Yeom, W. S. Yang, S. Hur, M. G. Kim, J. Im, J. Seo, J. H. Noh, S. I. Seok, 2017, "Colloidally prepared La-doped $BaSnO_3$ electrodes for efficient, photostable perovskite solar cells", *Science*, Vol. 356, pp. 167-171.

Snaith, H. J., 2013, "Perovskites: The Emergence of a New Era for Low-Cost, High-Efficiency Solar Cells", *The Journal of Physical Chemistry Letters*, Vol. 4, pp. 3623-3630.

Stranks, S. D., P. K. Nayak, W. Zhang, T. Stergiopoulos, and H. J. Snaith, 2015, "Formation of Thin Films of Organic–Inorganic Perovskites for High-Efficiency Solar Cells", *Angewandte Chemie International Edition*, Vol. 54, pp. 3240-3248.

Tian, H., B. Xu, H. Chen, E. M. J. Johansson, and G. Boschloo, 2014, "Solid-State Perovskite- Sensitized p-Type Mesoporous Nickel Oxide Solar Cells", *Chemistry & Sustainability*, Vol.7, pp. 2150-2153.

Tong, X., F. Lin, J. Wu, and Z. M. Wang, 2015, “High Performance Perovskite Solar Cells”, *Advanced Science*, Vol. 3, 1500201, pp. 1-18.

Tseng, Z., C. Chiang and C. Wu, 2015, “Surface Engineering of ZnO Thin Film for High Efficiency Planar Perovskite Solar Cells”, *Scientific Reports*, Vol. 5, 13211.

Ubani, C. A., M. A. Ibrahim, and M. A. M. Teridi, 2017, “Moving into the domain of perovskite sensitized solar cell”, *Renewable and Sustainable Energy Reviews*, Vol. 72, pp. 907-915.

Wang, J. T., J. M. Ball, E. M. Barea, A. Abate, J. A. Alexander-Webber, J. Huang, M. Saliba, I. Mora-Sero, J. Bisquert, H. J. Snaith, R. J. Nicholas, 2014, “Low-temperature processed electron collection layers of graphene/TiO_2 nanocomposites in thin film perovskite solar cells.”, *Nano Letters*, Vol. 2, pp. 724-730.

Wei, Q., Z. Yang, D. Yang, W. Zi, X. Ren, Y. Liu, X. Liu, J. Feng, S. (F.) Liu, 2016, “The effect of transparent conductive oxide on the performance $CH_3NH_3PbI_3$ perovskite solar cell without electron/hole selective layers”, *Solar Energy*, Vol. 135, pp. 654-661.

Xiao, Z., Y. Yuan, Q. Wang, Y. Shao, Y. Bai, Y. Deng, Q. Dong, M. Hu, C. Bi, and J. Huang, 2016, “Thin-film semiconductor perspective of organometal trihalide perovskite materials for high-efficiency solar cells”, *Materials Science and Engineering*, Vol. 101, pp. 1-38.

Yang, Y., J. Song, Y. L. Zhao, L. Zhu, X. Q. Gu, Y. Q. Gu, M. Che, and Y. H. Qiang, 2016, “Ammonium-iodide-salt additives induced photovoltaic performance enhancement in one-step solution process for perovskite solar cells”, *Journal of Alloys and Compounds*, Vol. 684, pp. 84-90.

Ye, M., X. Hong, F. Zhang and X. Liu, 2016, “Recent advancements in perovskite solar cells: flexibility, stability and large scale”, *Journal of Materials Chemistry A*, Vol. 4, pp. 6755-6771.

Yella, A., L.-P. Heiniger, P. Gao, M. K. Nazerruddin, and M. Grätzel, 2014, “Nanocrystalline rutile electron extraction layer enables low-temperature solution processed perovskite photovoltaics with 13.7% efficiency”, *Nano Letters*, Vol. 14, pp. 2591-2596.

You, J., Y. (M.) Yang, Z. Hong, T.-B. Song, L. Meng, Y. Liu, C. Jiang, H. Zhou, W.-H Chang, G. Li, and Y. Yang, 2014, “Moisture assisted perovskite film growth for high performance solar cells”, *Applied Physics Letters*, Vol. 105, p.183902.

You, J., L. Meng, T. Song, T. Guo, M. Yang, W. Chang, Z. Hong, H. Chen, H. Zhou, 2015, "Improved air stability of perovskite solar cells via solution-processed metal oxide transport layers", *Nature Nanotechnology*, Vol. 11, pp. 75–81.

Zhang, H., J. Cheng, F. Lin, H. He, J. Mao, K. S. Wong, A. K. Y. Jen, and W. C. H. Choy, 2015, “Pinhole-Free and Surface-Nanostructured NiOx Film by Room-Temperature Solution Process for High-Performance Flexible Perovskite Solar Cells with Good Stability and Reproducibility”, *American Chemical Society Nano*, Vol. 10, pp. 1503-1511.

Zhou, H., Q. Chen, G. Li, S. Luo, T. B. Song, H. S. Duan, Z. Hong, J. You, Y. Liu and Y. Yang, 2014, “Interface engineering of highly efficient perovskite solar cells”, *Science*, Vol. 345, pp. 542–546.

Zhu, Z., Y. Bai, T. Zhang, Z. Liu, X. Long, Z. Wei, Z. Wang, L. Zhang, J. Wang, F. Yan, and S. Yang, 2014, “High-performance hole-extraction layer of Sol–Gel-Processed NiO nanocrystals for inverted planar perovskite solar cells.”, *Angewandte Chemie International Edition*, Vol. 53, pp. 12571-12575.